RNA BIOLOGY
2025, VOL. 22, NO. 1, 1–18
https://doi.org/10.1080/15476286.2025.2515655

Taylor & Francis
Taylor & Francis Group

RESEARCH ARTICLE

OPEN ACCESS Check for updates

Systematic analysis of A-to-I RNA editing upon release of ADAR from the nucleolus

Ruben Lattuca[a,b], Rümeyza Bascetin[a], Vincent Detours[b*], and Denis L. J. Lafontaine [a*]

[a]RNA Molecular Biology, Fonds de la Recherche Scientifique (F.R.S./FNRS), Université libre de Bruxelles (ULB), Biopark campus, B-6041 Gosselies, Belgium; [b]IRIBHM Jacques E. Dumont, Université libre de Bruxelles, Lennik, Belgium

ABSTRACT

Adenosine-to-inosine (A-to-I) RNA editing, catalysed by two ADAR isoforms (p110 and p150) and ADARB1, is a critical regulatory step in gene expression. Intriguingly, the nucleolus is conspicuously rich in ADAR p110 and ADARB1, though the biological reason remains unclear. To investigate a putative role of nucleolar enrichment in ADAR, we released it gradually from the nucleolus into the nucleoplasm by treating cells briefly with low doses of actinomycin D, known to disassemble the nucleolus. Deep sequencing of the transcriptome revealed that as ADAR dissociated from the nucleolus, RNA editing increased significantly, with sharp rises in both the number of edited sites and editing frequency. This co-transcriptional editing, predominantly in intronic regions, was associated with disrupted pre-mRNA splicing, causing exon skipping and intron retention which remodelled gene expression. These findings suggest that the nucleolar localization of ADAR serves to restrain its activity, preventing excessive editing that could lead to splicing errors and cellular dysfunction.

ARTICLE HISTORY
Revised 18 May 2025
Accepted 23 May 2025

KEYWORDS
A-to-I RNA editing; ADAR; nucleolus; RNA modification; epitranscriptomics; pre-mRNA splicing regulation

Introduction

Adenosine deaminases acting on RNA (ADAR) binds to double-stranded RNAs (dsRNAs), where they may convert adenosines to inosines, which are structurally similar to guanosine [1–3]. No less than 4.5 million editing sites have been identified in metazoans [4]. Most editing events occur in repeats of Alu, a pervasive repetitive element prone to form double stranded structures [5–9].

There are two isoforms of ADAR: p110, which is constitutively produced and active in the nucleoplasm, and p150, which is induced by interferon and active mainly in the cytoplasm, though it shuttles between the cytoplasm and the nucleus [10–12]. In addition, there are two paralogs: ADARB1 and ADARB2. The nuclei of brain cells are highly enriched in both ADAR and ADARB1 [13–16]. ADARB2 is an editing-inactive enzyme produced exclusively in the brain and which may play a role in regulating RNA editing [17–21].

A-to-I editing is involved in regulating key biological processes such as pre-mRNA splicing, RNA stability, and translation [22–25] and the interferon response against dsRNAs [10,26,27]. Regulation of the interferon response is essential to organism survival. ADAR inhibition or loss of function in mouse leads to embryonic lethality with an aberrant immune response [28]. In human, ADAR mutations cause Aicardi-Goutières syndrome, an inflammatory neuronal disorder associated with increasing type I interferon activity [27].

The nucleolus is a multilayered biomolecular condensate, formed by liquid–liquid phase separation, where the initial steps of ribosome biogenesis take place [29]. The nucleolar proteome contains many proteins with no obvious relationship to ribosome biogenesis, including isoforms of ADAR [30–32]. The presence of non-ribosomal proteins in the nucleolus reflects its involvement in diverse, apparently unrelated processes essential to maintaining cell homoeostasis. The nucleolus consists of three main nested layers: the fibrillar centre (FC), the dense fibrillar component (DFC), and the granular component (GC), whose precise spatial juxtaposition relies on ongoing ribosome biogenesis [29]. When pre-rRNA synthesis is blocked by treating cells with an RNA polymerase I inhibitor (e.g. actinomycin D), the nucleolus is progressively disassembled. This leads to a complete redistribution of nucleolar proteins, with the formation of remarkable nucleolar 'caps' (see Figure 1A, see FBL panel 90 min, green arrowheads).

A significant fraction of ADAR, including p110 and ADARB1, has been observed in the nucleolus in cells of different origins (brain, breast, and cervix), in multiple organisms (fly, rat, and human), and in both normal and pathological contexts, including cancer [16,20,30,32–37]. This may be surprising, as most ADAR substrates are expected to reside within the nucleoplasm. Several observations indicate that ADAR shuttles between the nucleolus and nucleoplasm

CONTACT Vincent Detours vincent.detours@ulb.be IRIBHM Jacques E. Dumont, Université libre de Bruxelles, CP602 808 route de Lennik, B-1070 Brussels, Belgium; Denis L. J. Lafontaine denis.lafontaine@ulb.be RNA Molecular Biology, Fonds de la Recherche Scientifique (F.R.S./FNRS), Université libre de Bruxelles (ULB), Biopark Campus, B-6041, Belgium
*Equal contribution, co-lead.

Supplemental data for this article can be accessed online at https://doi.org/10.1080/15476286.2025.2515655

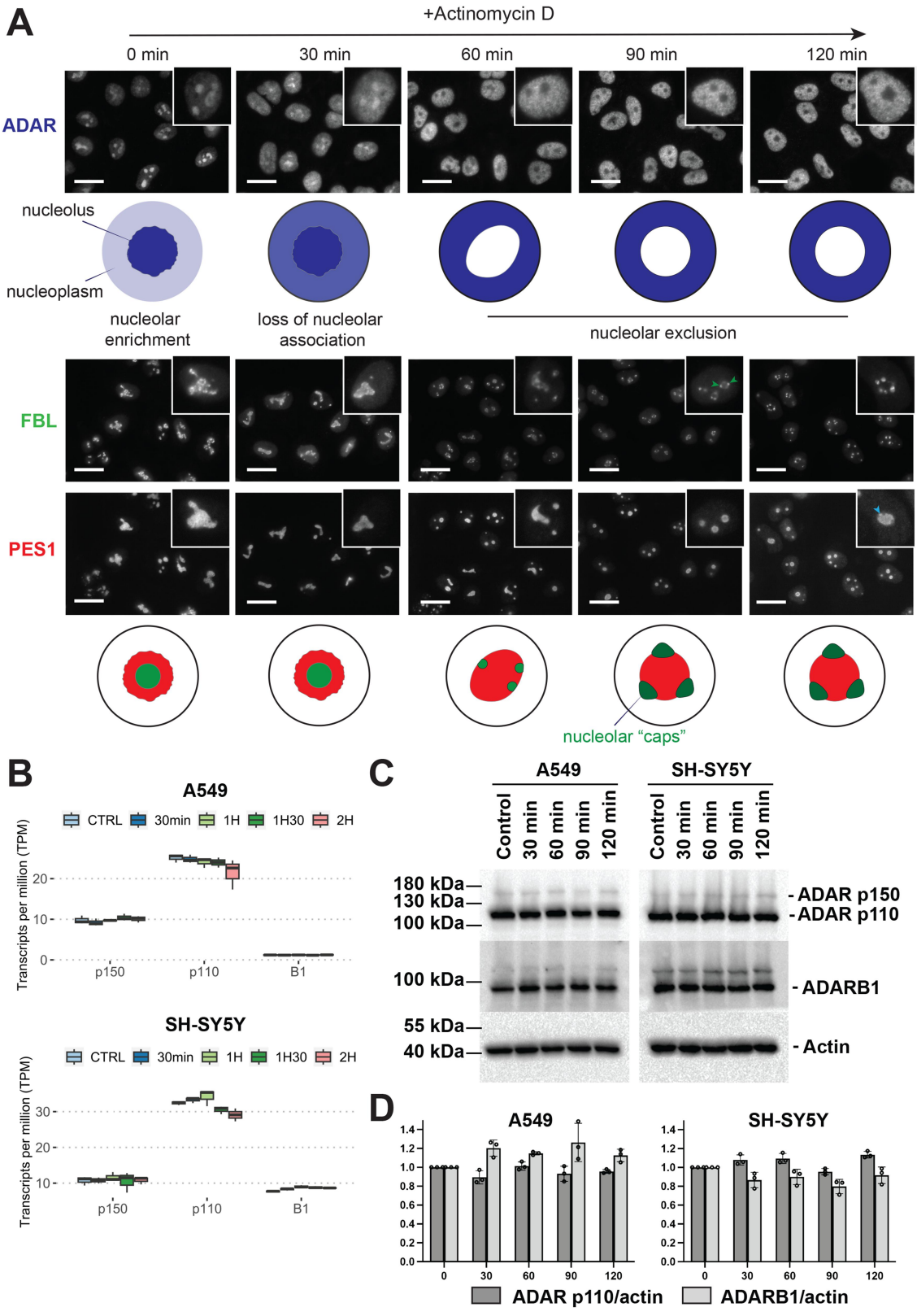

Figure 1. Nucleolar disassembly leads to gradual release of nucleolar ADAR into the nucleoplasm A) Rationale. The gradual dissociation of ADAR from the nucleolus was prompted by disassembly of the nucleolus triggered by treatment of cells with a low dose of actinomycin D (Act D, 0.1 µg/ml). The figure depicts the different distribution patterns of ADAR observed: marked nucleolar enrichment (0 min), progressive loss of nucleolar association, with partial redistribution to the nucleoplasm (30 min), and full redistribution of ADAR to the nucleoplasm and near complete exclusion from the nucleolus (60, 90, and 120 min). For reference, fibrillarin (FBL) and pescadillo 1 (PES1) were used, respectively, as markers of an internal and a peripheral layer of the nucleolus. As the nucleolus disassembles, FBL is redistributed to the periphery of the organelle, forming foci that coalesce in "caps". Representative nucleolar caps are highlighted with green arrowheads. Immunostaining of A549 cells with antibodies specific to ADAR or to the nucleolar marker FBL or PES1. Insets, show a zoomed in cell. Scale bar, 20 µm. For colocalization and for the same analysis on SH-SY5Y cells, see Supplemental Figure 1. B) mRNA levels. Levels of ADAR-isoform (p110 and p150) and ADARB1 transcripts (in transcripts per million, TPM) for each condition in A549 and SH-SY5Y. ADAR p110 is the most expressed isoform in both cell lines and is slightly more expressed in SH-SY5Y (25 and 35 TPM in A549 and SH-SY5Y, respectively). ADAR p150 expression is similar in the two cell lines (10 TPM). ADARB1 expression is low in A549 (2 TPM). C) Protein level. Steady-state levels of ADAR upon Act D treatment. Total protein extracted from the indicated cell lines was analysed by western blotting with antibodies specific to ADAR or ADARB1. As loading control, actin probing was used. D) The levels of ADAR p110 and ADARB1 in A549 and SH-SY5Y cells during Act D treatment were quantified using a Chemidoc and normalized to actin (n = 3). The data show only marginal variation.

[30,32,35]. Firstly, fluorescence recovery after photobleaching (FRAP) has revealed in HeLa cells that the association of ADAR and ADARB1 with the nucleolus is dynamic [30,32,35]. Secondly, upon overexpression of ADAR substrates in the nucleoplasm, both ADAR and ADARB1 have been shown to be redistributed from the nucleolus to the nucleoplasm [30]. How this might affect global editing has not been investigated.

The presence of ADAR p110 and ADARB1 in the nucleolus begs the question of whether these enzymes edit RNAs there. Apparently this is not the case, as nucleolar RNAs, including pre-rRNAs and snoRNAs, are not obviously edited (this work and [30]). This is interesting, as ADAR can function in the nucleolus if substrates normally present in the nucleoplasm are artificially targeted to it [31]. Additional connections between ADAR and the nucleolus have recently been provided by characterizing its interactome by affinity purification or proximity labelling experiments followed by mass spec analysis [38–40]. This revealed that ADAR and ADARB1 interact with numerous nucleolar proteins including, abundant scaffold proteins such as nucleolin (NCL), nucleophosmin (NPM1), and others in different cell types [38–40]. The significance of these putative interactions remains unknown.

Here, as an initial approach to understanding why the nucleolus is enriched in ADAR, we have released it gradually into the nucleoplasm by disassembling the organelle and then used deep transcriptome sequencing to assess the impact of this release on global RNA editing. We reveal that releasing ADAR from the nucleolus mimics ADAR overexpression, leading to an increased number of edited sites and an increased editing frequency. This increased editing leads to aberrant pre-mRNA splicing, including exon skipping and intron retention. These results underscore the physiological significance of nucleolar localization in regulating ADAR activity and the importance of maintaining a functionally intact nucleolus.

Results

Nucleolar disassembly leads to gradual release of ADAR from the nucleolus into the nucleoplasm

Why the nucleolus is significantly enriched in ADAR remains poorly understood. We reasoned that one way to address this question would be to release ADAR gradually from the nucleolus by disassembling it, and then to characterize RNA editing globally by sequencing the entire transcriptome.

To disassemble the nucleolus, we chose to expose cells briefly to a low dose (0.1 μg/ml) of actinomycin D (Act D), a compound which inhibits only RNA polymerase I (Pol I) at this concentration [41]. In the absence of pre-rRNA synthesis, the nucleolus is gradually disassembled [42,43]. Importantly, at this concentration of Act D, only Pol I is affected, while Pol II and Pol III remain unaffected, as they are inhibited only at concentrations above 0.5 μg/ml and 5 μg/ml, respectively, as discussed in Ref [44].

The nucleolar disassembly assay was carried out in two cell lines: A549, derived from a human alveolar adenocarcinoma, and SH-SY5Y, derived from a neuroblastoma. Actinomycin D-treated cells were harvested after 30, 60, 90, and 120 min of treatment. As a control, cells were also collected prior to treatment. To monitor the subcellular distribution of ADAR and gradual disassembly of the nucleolus, we performed immunostaining with antibodies specifically recognizing ADAR (ADAR and ADARB1 were tested individually) or the nucleolar marker fibrillarin (FBL) or pescadillo 1 (PES1). FBL detects an internal layer of the nucleolus, the dense fibrillar component (DFC) [45]. PES1 labels a peripheral layer of the nucleolus, the granular component (GC) [46]. In Figure 1A, ADAR was stained separately, and FBL and PES1 were co-detected to illustrate that the GC subcompartment of the nucleolus surrounds the DFC. In Figure S1, ADAR (or ADARB1) and PES1 were co-stained, and FBL was stained separately.

First, we confirmed in untreated cells of both cell lines the strong enrichment of ADAR in the nucleolus (0 min time point) (Figure 1A, Figure S1). ADARB1 was detected in the nucleolus of untreated SH-SY5Y cells (Figure S1) but not in those of A549 cells (even though it is apparently expressed similarly in both cell types, see Figure 1B-C). In untreated cells, FBL and PES1 were distributed, respectively, as expected for an internal and a peripheral nucleolar protein.

After 30 min of treatment, the localization of the nucleolar proteins started to change: FBL was redistributed, initially concentrating in small foci that progressively localized to the periphery of the organelle, forming 'caps' which were conspicuous from 90 min of treatment onward (see green arrowheads in Figure 1A). The phase behaviour of PES1 was also altered. In the steady state, the protein was evenly distributed through the GC, which appeared irregular, with a rugged contour. As the time course of Act D treatment progressed, the GC adopted a more regular shape, initially ovoid and ultimately spherical, displaying more intense PES1 staining at the periphery, where it formed a punctuate ring (Figure 1A, blue arrowhead).

In parallel, ADAR gradually lost its association with the nucleolus. At 30 min, a large fraction of ADAR was detected in the nucleoplasm. At 60 min and later, ADAR was nearly completely excluded from the nucleolus and detected only in the nucleoplasm. A549 and SH-SY5Y cells showed similar kinetics of ADAR dissociation from the nucleolus (Figure S1). In SH-SY5Y, where ADARB1 was detectable, it was also relocated gradually to the nucleoplasm (Figure S1).

We then assessed by RNAseq the abundance of mRNAs encoding ADAR p110, ADAR p150, and ADARB1 in A549 and SH-SY5Y cells (Figure 1B). In both cell models, we found the mRNA of the p110 isoform to be considerably more abundant than that of p150. ADARB1 expression appeared much lower. We will therefore assume in what follows that the described effects on editing of ADAR release from the nucleolus were largely attributable to p110. At the protein level, use of an antibody detecting the p110 and p150 isoforms confirmed that p110 is far more abundant. An antibody specific to ADARB1 confirmed its presence (Figure 1B).

Next, we established whether Act D treatment affected in any way the expression of ADAR in cells. RNAseq analysis

revealed that neither ADAR p110, ADAR p150, nor ADARB1 expression was affected over the time course of treatment (Figure 1B, Figure S2, q-values >0.18, q is a multiple-testing-corrected measure of statistical significance). In addition, Western blotting and quantitative analysis showed that the corresponding protein levels remained largely unaffected over the 2-h course of the experiment (Figure 1C-D).

In conclusion, it was possible to release ADAR gradually from the nucleolus into the nucleoplasm by disassembling the condensate by treating cells briefly with a drug that inhibits rRNA synthesis.

Release of ADAR from the nucleolus increases editing

To assess globally how ADAR redistribution from the nucleolus to the nucleoplasm affects editing, we performed transcriptome-wide sequencing of total RNA fractions. In practice, total RNA was extracted at each time point of the nucleolar disassembly discussed above, processed into libraries and subjected to deep sequencing. We systematically investigated 1) the number of edited sites and 2) the fraction of edited reads at each edited site (Figure 2A). All assays were performed in biological triplicates to ascertain the reproducibility of our observations.

We mapped systematically all detected edited sites in the transcriptome in regions sequenced with a coverage depth >10×. We filtered out potential sequencing and mapping errors with the REDItools suite [47] and eliminated the single nucleotide variants known in A549 [48] and SH-SY5Y [49].

As a quality control step, we assessed the overlap between the editing sites detected in our dataset and those listed in REDIportal, a comprehensive database of A-to-I editing [4]. At a minimum coverage of 10×, we detected up to 73% of REDIportal-listed sites in A549 cells and up to 72% in SH-SY5Y cells (Figure S3A). Increasing the coverage threshold to 20×—which reduces the number of false positives – raised these percentages to 87% for A549 and 82% for SH-SY5Y (Figure S3B). At 30× coverage, the overlap further increased to 91.5% for A549 and remained at 82% for SH-SY5Y (Figure S3C). Thus, even at 10× coverage, the overlap with REDIportal was substantial and improved with more stringent coverage thresholds. For all subsequent analyses, we used our internally defined and validated map of edited sites.

A principal component analysis (PCA) of editing frequencies throughout nucleolar disassembly revealed excellent clustering of triplicates along PC1 for each Act D treatment time (Figure S4A, 67% and 64% of variance explained in A549 and

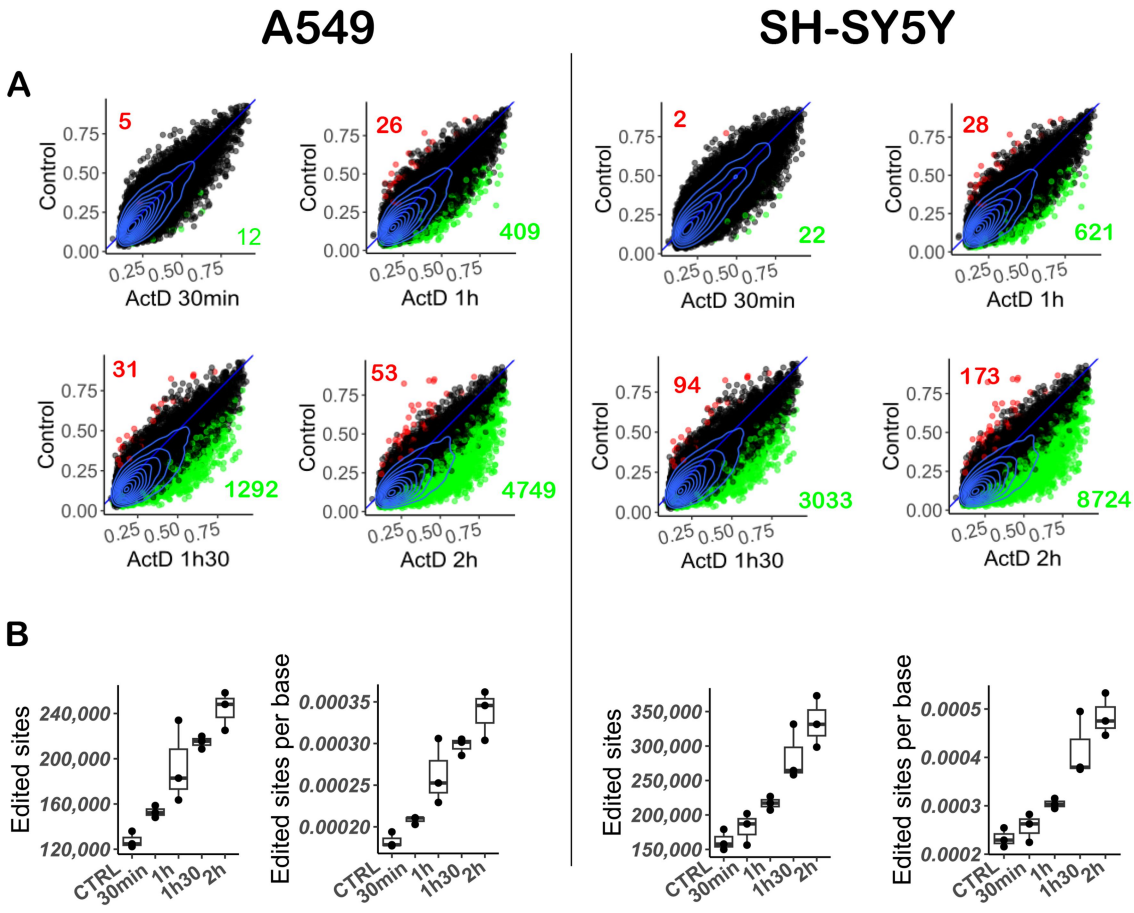

Figure 2. Effect of nucleolar disassembly on editing frequency and the number of edited sites A) Comparison of editing frequencies in A549 and SH-SY5Y cells after 30 min (top left), 1 h (top right), 1.5 h (bottom left), and 2 h (bottom right). Black, green, and red dots respectively indicate, for each treatment time, the edited sites with no significant change in editing frequency, a significant increase, or a significant decrease as compared to untreated cells. Edited sites were selected with a ≥ 10x coverage and detected in each replicate for each condition. A Fisher test was performed on the mean proportion of adenosine converted to guanosine in order to assess the significance of differentially edited sites (q-value <0.05, q is a multiple-testing-corrected measure of statistical significance). B) Number of edited sites (left) and edited sites per base (right) in A549 and SH-SY5Y cells for each treatment time and for untreated cells. For changes in the number of edited sites, see main text. For number of edited sites per base: After 30 minutes, we observed an average increase of 16% in A549 and of 12% in SH-SY5Y compared to untreated cells. In 2 h-treated cells, it was a 1.84 and 2.1-fold increase in A549 and SH-SY5Y, respectively.

SH-SY5Y cells, respectively) and a very good separation of the groups in PC2. This attests to the robustness of our approach. The samples were also clustered nicely when gene expression was analysed in a PCA (Figure S4B).

For both cell lines, we computed the differential editing frequency of commonly edited sites between untreated cells and each treatment duration and observed a steady increase over treatment time (Figure 2A).

After 30 min of treatment, as ADAR started to be released from the nucleolus into the nucleoplasm, we detected 12 and 22 sites with significantly increased editing frequency (q-value <0.05) in A549 and SH-SY5Y, respectively. After 1 h, a significant increase in editing frequency was detected at 409 and 621 sites (q-value <0.05) in A549 and SH-SY5Y, respectively. After 1h30, we observed an increase in editing frequency at 1292 sites in A549 and 3033 sites in SH-SY5Y (q-value <0.05). After 2 h, 4749 and 8724 sites showed significantly increased editing.

We also observed some decreased editing frequencies, but at much fewer sites. There was an increase in such events over time, culminating (at 2 h actinomycin treatment) at 53 sites in A549 cells and 173 sites in SH-SY5Y cells (q-value <0.05), representing 1% and 2% of the total differentially edited sites.

Thus, for sites showing a variation (increase or decrease) in editing frequency, we noted a gradual effect correlating well with progressive release of ADAR from the nucleolus into the nucleoplasm (Figure 1A).

We next counted the number of edited sites and normalized it to the number of bases covered at ≥10× in untreated and treated cells (Figure 2B). On average across replicates we detected 127,600 and 162,300 edited sites in untreated A549 and SH-SY5Y cells, respectively. After 30 min of treatment, we observed an average 20% increase in the number of edited sites in A549 cells and 12% in SH-SY5Y as compared to untreated cells (Figure 2B). After 2 h of treatment, we observed an increase in the number of edited sites to 244,000 in A549 cells and 334,000 in SH-SY5Y cells. These numbers represent, respectively, a 1.9 and a 2.1-fold increase as compared to the corresponding untreated control cells (Figure 2B).

In conclusion, the gradual release of ADAR from the nucleolus is accompanied by a marked increase in edited site number and editing frequency. Interestingly, these effects mimic, to some extent, those reported upon the overexpression of ADAR [33] (See Discussion, see Figure S15).

To ensure a comprehensive analysis, we computed all the 12 possible RNA-DNA differences across each triplicate for each time point in both cell lines (Figure S5).

This analysis confirmed that the predominant RNA-DNA mismatches are A-to-G and T-to-C, which correspond to ADAR-mediated editing, and that their frequencies steadily increase during the experiment. Specifically, in A549 cells, the proportions of A > G and T > C changes increased from 23.17% to 30.12% and from 22.68% to 29.76%, respectively, after 2 h of treatment. In SH-SY5Y cells, these proportions increase from 24.11% to 33.65% and from 24.1% to 33.1%, respectively (Figure S5B).

We also observed that the second most frequent RNA-DNA differences were C-to-T and G-to-A, consistent with APOBEC-mediated editing. Notably, these remained constant throughout the experiment, providing an additional specificity control for our experimental design.

The remaining eight mismatch types (A > C, A > T, C > A, C > G, G > C, G > T, T > A and T > G) were detected at much lower frequencies. Assuming these represent false positive, we estimated the false-positive rates for A-to-G and T-to-C site detection to be of 3% and 2.7% in A549 and SH-SY5Y, respectively.

Finally, we compared the variation in proportions for all mismatch types between control and 2 h-treated cells. Only A >G and T > C differences showed significant increases (Fisher's exact test with Benjamini–Hochberg correction for multiple testing: A549-adjusted p-values = 5.34×10^{-23} and 7.68×10^{-23} for A > G and T > C increases, respectively; SH-SY5Y -adjusted p-values = 1.43×10^{-73} and 6.53×10^{-48}, respectively).

Complete datasets for 'edited sites' and 'differentially edited sites' are provided in Table S1 and Table S2.

ADAR p110 up-regulates the editing level co-transcriptionally

The editing activity of ADAR p110 is thought to occur in the nucleoplasm, and that of ADAR p150 in the cytoplasm. Recently, it was reported that ADAR p110 exerts its editing activity mostly on intronic and repetitive regions, while ADAR p150 mostly edits 3' untranslated regions (UTRs) and exonic regions, at least in mouse embryonic fibroblasts (MEFs) [50]. Additionally, in agreement with their reported substrate preferences in MEFs, RIP-sequencing analysis in HEK293 cells has revealed that ADAR p110 binds primarily to intronic regions, while ADAR p150 is mostly associated with exonic regions and 3' UTRs [50]. As discussed above, the p110 form is dominant in our cells (Figure 1B–C). We therefore predicted that nucleolar disassembly would mostly affect editing of introns and repetitive elements.

To test our prediction, we computed the distribution of edited sites in 'genes' and repetitive elements (Figure 3A). For the 'gene' analysis', we distinguished 5' and 3' UTR regions, coding sequence (CDS), introns, and intergenic regions; for the 'repetitive element' analysis, we considered the long interspersed nuclear elements (LINE), short interspersed nuclear elements (SINE – containing the heavily edited Alu elements), and long terminal repeats (LTR) elements. We used as cut-off the presence of edited sites in at least two samples of the triplicate with a ≥10× coverage.

In both cell models, we did find editing to occur mainly in intronic regions and SINEs (Figure 3A). This trend remained unchanged upon nucleolar disassembly. Specifically, upon nucleolar disassembly, the editing of intronic regions increased from 75% to 82% in A549 and from 74% to 83% in SH-SY5Y (2-h time point, Figure 3A). Similarly, the editing of SINE regions increased from 77% to 83% and from 75% to 82% in the A549 and SH-SY5Y cell lines, respectively (2-h time point, Figure 3A).

As discussed in detail later in the manuscript (see Figure 5), the increased editing observed following the nucleolar release of ADAR leads to aberrant splicing,

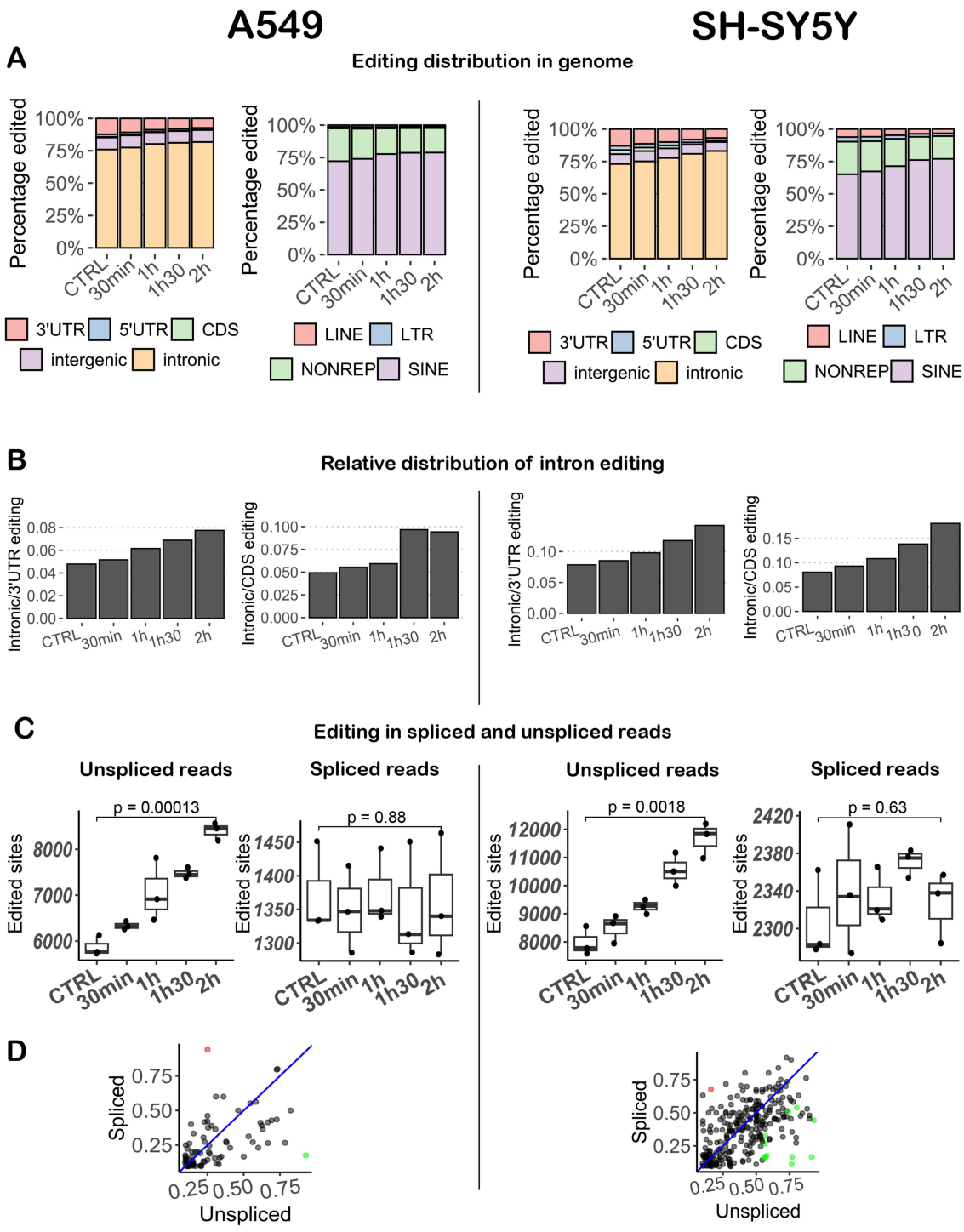

Figure 3. Substrate distribution of ADAR editing upon ADAR release from the nucleolus A) Distribution of editing among transcribed gene regions (left) and transcribed repetitive regions (right) in A549 and SH-SY5Y. Edited sites detected with coverage ≥ 10x and in at least two replicates for each condition were included in this tally. Editing occurs mostly in intronic and SINE regions and both proportions increase upon actinomycin treatment. B) Ratio of the number of edited sites per base in intronic versus 3' UTR regions (left) and in intronic versus CDS regions (right) in A549 and SH-SY5Y. Editing ratios increase with treatment time, suggesting intronic editing as the major contribution to editing. C) Edited sites in 'unspliced reads' (left) and 'spliced reads' (right). A significant increase in editing is observed in unspliced reads during Act D treatment, but not in spliced reads (p-values = 0.88, 0.63). D) The scatter plots depict the editing frequency of edited sites shared between spliced and unspliced reads. Most sites (~97%) show no difference in editing frequency between the spliced and the unspliced read (q-values > 0.05), which indicates that editing occurred before splicing.

including intron retention. However, with only 97 occurrences in A549 and 192 in SH-SY5Y cells (Figure 5A), intron retention events were limited and cannot account for the observed increase in editing.

Indeed, when we compared the number of edited sites in genes with differentially retained introns after 2 h of actinomycin D treatment (editing frequency ≥0.1, coverage ≥10×, edited sites detected in at least two of three triplicates;

Figure S6), we found only 749 and 2,953 edited sites in genes with retained introns in A549 and SH-SY5Y cells, respectively (Figure S6). These represent just 0.75% and 1.75% of the total edited sites at 2 h treatment.

We conclude that the increase in editing is not attributable to editing within retained introns.

As ADAR p110 editing activity is thought to be largely nucleoplasmic and to target introns, the increased editing due to ADAR release from the nucleolus should in principle occur mostly co-transcriptionally, on nascent RNAs. We therefore computed the ratios of intronic-versus-CDS and intronic-versus-3'-UTR editing to assess the contribution of ADAR p110 as compared to ADAR p150 (the latter is expected to work mostly in the cytoplasm and is also far less abundant in our cells, see Figure 1C). The number of edited sites detected were normalized to the lengths of the relevant sequence types, as intronic regions tend to be longer than 3'-UTR and coding regions.

After 2 h of Act D treatment, the A549 cell line showed a 1.62-fold increase in the intronic/3'-UTR editing ratio and a 2-fold increase in the intronic/CDS editing ratio (Figure 3B). For the SH-SY5Y cell line, the ratio increases were respectfully 1.81- and 2.24-fold (Figure 3B). We conclude that the editing increase occurs mostly in the nucleoplasm and in introns, where it is carried out by the abundant ADAR p110.

Along the same line, we quantified editing in 'spliced reads', i.e. reads overlapping with exon–exon junctions, and 'unspliced reads', i.e. reads overlapping with exon-intron junctions (Figure 3C). In both cell lines, editing was found to increase significantly over time in 'unspliced reads' (p-values = 0.00013 in A549, p-values = 0.018 in SH-SY5Y) but not in 'spliced reads' (p-values = 0.88 and 0.63) (Figure 3C). When compared in cells treated for 2 h, sites common to 'spliced' and 'unspliced' reads showed no significant difference in editing frequency (q-values >0.05). This suggests that 'unspliced reads' are already edited before RNA processing (Figure 3D, bottom).

Altered editing leads to monotonous variation in gene and isoform expression

Editing by ADAR regulates both co- and post-transcriptional mRNA maturation processes [22–25]. To assess the impact of ADAR release from the nucleolus, we first compared gene and isoform expression in 2-h-treated versus untreated cells (Figure 4).

First, 161 and 192 differentially expressed genes (DEGs, $|\log_2 FC| \geq 1$ and q-value <0.01) were detected after 2-h treatment in A549 and SH-SY5Y, respectively (Figure 4A, left). While there was a general bias towards down-regulation, 42% (A549) and 33% (SH-SY5Y) of the affected genes were up-regulated.

We next turned our attention to differentially expressed isoforms (DEI). We observed 1116 and 1619 DEIs ($|\log_2 FC| \geq 1$, q-value ≤0.01) in A549 and SH-SY5Y, respectively (Figure 4A, middle). We investigated whether the magnitude of the fold change might also be significantly greater for DEIs than for DEGs, and we observed it is the case. In A549 and SH-SY5Y, respectively, we observed a mean $|\log_2 FC|$ of 0.4 and 0.41 for genes versus 0.68 and 0.73 for isoforms (Figure 4A, right), both being significant (p-value $<2.2 \times 10^{-16}$). This highlights the potential regulation of alternative splicing.

While genes and isoforms displayed differential expression after 2 h of treatment, their expression might imaginably vary non-monotonously in the course of treatment. We thus plotted over time the expression of all genes (Figure 4B), or all isoforms (Figure 4C), meeting the criteria $|\log_2 FC| \geq 1$, q-value ≤0.01 after 2 h of treatment. In both cell lines, we observed a strikingly monotonous variation of the expression of both up- and down-regulated genes and isoforms, in line with the gradual nucleolar alteration and variations in editing.

Complete datasets for 'differentially expressed genes' and 'differentially expressed isoforms' are provided in Table S3 and Table S4.

As discussed above, the low concentration of Act D used in this study (0.1 µg/ml) was specifically chosen because it selectively inhibits RNA polymerase I (Pol I), while higher concentrations are required to inhibit Pol II and Pol III (>0.5 µg/ml and >5 µg/ml, respectively) [44]. Under our experimental conditions, only 92 and 128 genes were repressed after 2 h of Act D treatment in A549 and SH-SY5Y cells, respectively (Figure 4A). This modest transcriptional repression should be viewed in the context of the thousands of sites that exhibited increased editing during the treatment.

To further support this point, we compared the effect of a 2-h treatment with either a low (0.1 µg/ml) or high (5 µg/ml) concentration of Act D on gene expression (Figure S7). The results showed: (1) a tenfold increase in the number of repressed genes at the higher dose (Figure S7A); and (2) that at the low dose, fewer than 1% of expressed genes were affected (Figure S7B).

In conclusion, the low concentration of Act D used here had only minimal impact on the transcriptome and mRNA stability – an effect that stands in sharp contrast to the widespread changes observed at the higher dose of 5 µg/ml.

Enrichment in intronic editing may regulate alternative pre-mRNA splicing

Next, we investigated whether alternative or aberrant splicing events might be associated with the types of changes in RNA editing observed upon release of ADAR from the nucleolus. For simplicity, we compared the 2-h treatment time point with untreated cells.

The software rMATS [51] was used to detect differential alternative splicing events between 2-h-treated and untreated cells. The events considered were: skipped exons, retained introns, alternative 5' splice sites, alternative 3' splice sites, and mutually exclusive exons.

The main differential splicing events observed in our datasets were exon skipping and inclusion (SE) and intron retention (RI) events (Figure 5A). No less than 150 SE and 97 RI events were detected in A549 cells and 200 SE and 192 RI events in SH-SY5Y cells (q-values <0.05). These changes were monotonous over treatment time (Figure S8). There was also some occurrence of alternative 5' or 3' splice sites and of

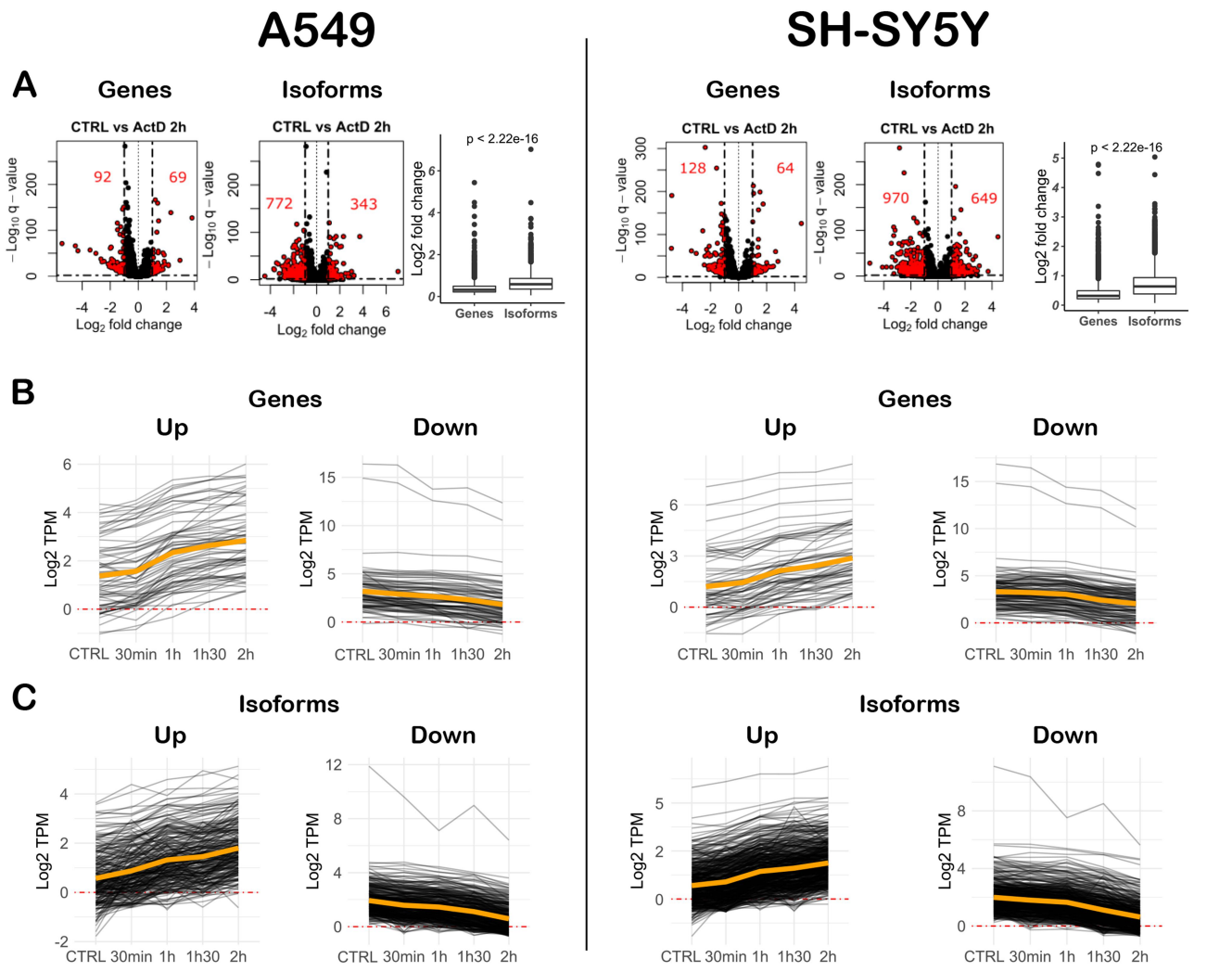

Figure 4. The effects of nucleolar disassembly on the transcriptome are monotonous A) Differentially expressed genes and isoforms in A549 and SH-SY5Y cell lines, respectively (red depicts $|\log_2 FC| \geq 1$, q-value 0.01). Boxplots compare the absolute log2 fold changes in transcript levels. B) Variation of gene expression (transcripts per million, TPM) in A549 and SH-SY5Y cells in the course of Act D treatment. In each pair of panels, genes selected for $|\log_2 FC| \geq 1$, q-value <0.01 are separated between left panel and right according to the sign of expression fold-change after two hours of Act D treatment. Expression either increases or decreases monotonously over the duration of the treatment. C) Same as panel B) for isoforms.

mutually exclusive exons, but these were far less numerous (Figure 5A).

Previous studies have concluded that exon skipping and exon inclusion events might be regulated by intronic editing [23,25]. We thus assessed editing in genes identified as differentially spliced and then examined where editing took place: was it in an intron or not, and if so, was the intron next to the skipped/included exon or not? We also looked at the distance between edited sites and splice junctions.

First, we compared the number of edited sites per base in transcripts undergoing exon skipping or inclusion (classified as 'aberrant') versus those that did not (classified as 'normal') (Figure 5B, q-value <0.05). In A549 and SH-SY5Y, aberrantly spliced transcripts were found to be 1.26-fold and 1.65-fold more edited, respectively, than their non-aberrant counterparts (p-values $<2.2 \times 10^{-16}$)(Figure 5B).

Next, we examined the number of edited sites per base in intronic regions flanking aberrantly skipped or included exon ('aberrant') compared to those flanking normally spliced exons ('normal') (Figure 5B). In A549 and SH-SY5Y cells, introns adjacent to aberrantly spliced exons were 2.5-fold and 3.48-fold more enriched in edited sites, respectively (p-values $<2.2 \times 10^{-16}$, Figure 5B). We then analysed individual transcripts by comparing the mean number of edited sites per base in introns flanking aberrantly spliced exons. Consistent with our previous results, we observed a significant increase in editing in these regions (p-values = 6.99×10^{-6}, 6.53×10^{-6}, Figure S9).

Finally, we assessed the distance (in nucleotides) between edited sites and their nearest splice junctions (Figure S10). We observed subtle effects, including a slight increase in the mean distance between the nearest edited site and the splice junction (Figure S10A), as well as increased editing at the splicing sites flanking the junction (Figure S10B). These changes appeared to reflect a global increase in editing rather than a specific alteration at the junction itself (Figure S10C).

We conclude that the observed increase in editing is a global effect that does not localize specifically to splice sites. We propose that splicing alterations may be driven by editing events located several kilobases away from the splice

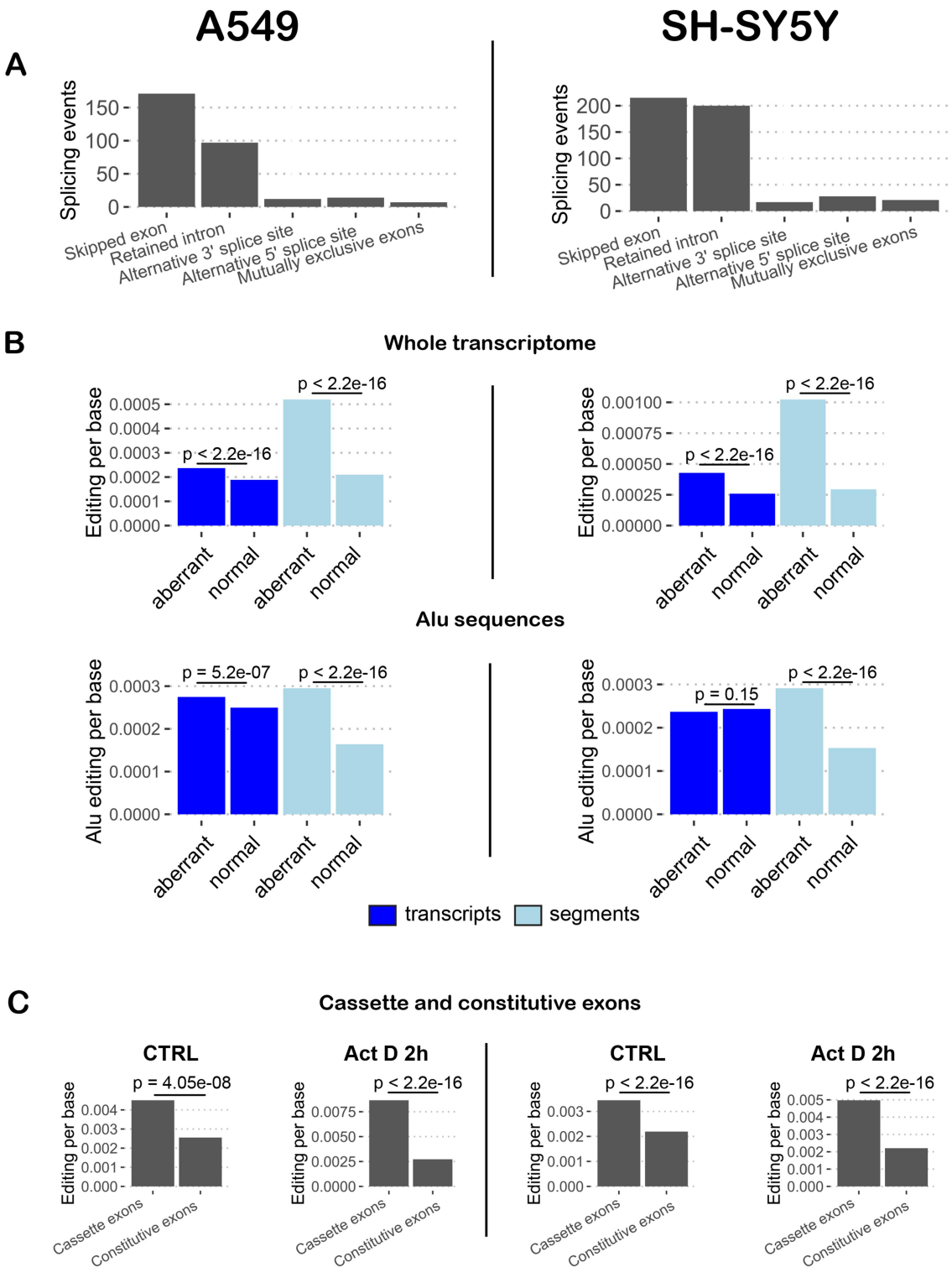

Figure 5. Regulation of exon skipping and inclusion events is editing-dependent A) Differential alternative splicing between untreated cells and cells treated for 2 h with Act D, according to the type of alternative splicing event indicated. Results computed with rMATS (q-values < 0.05). B) Number of edited sites per base (i.e., normalized to gene or segment length) computed for exon-skipping and exon-inclusion events (events detected in at least two replicates at coverage ≥ 10x) in transcripts showing altered ('aberrant') exon skipping/inclusion or not ('normal') and in 'segments' defined as intronic sequences flanking or not an aberrantly skipped or included exon (median intron length = 2 kb). Segments flanking aberrantly skipped or included exons are significantly richer in editing events. Numbers of Alu elements per base (i.e., normalized to gene or segment length) are also higher in segments flanking aberrantly skipped or included exons (bottom). C) Numbers of edited sites per base (i.e., normalized to cassette or constitutive exon length, respectively) are compared between cassette exons (exons that may be spliced out) and constitutive exons (constitutively included exons) in control and 2-hour treated A549 or SH-SY5Y cells (editing events detected in at least two replicates at coverage≥ 10X). Editing levels are significantly higher in cassette exons in both control (CTRL, p-values < 2.2x10-16) and 2-hour-treated cells (Act D 2h, p-values < 2.2x10-16).

junction, potentially through the formation of secondary or tertiary RNA structures.

Because Alu elements are particularly prone to A-to-I editing, we next examined whether the transcripts or intronic segments labelled as 'aberrant' in Figure 5B might be richer in Alu than those labelled as 'normal'.

In SH-SY5Y cells, transcripts with aberrant exon skipping/inclusion events displayed no enrichment in Alu as compared to transcripts with a normal exon skipping/exclusion pattern (p-values = 0.15), but an 1.14-fold enrichment was observed in A549 cells. In both A549 and SH-SY5Y cells, we found intronic sequences flanking aberrantly skipped or included exons to be significantly richer in Alu (respectively, 1.8-fold and 2-fold) (p-values $<2.2 \times 10^{-16}$, Figure 5B). Thus, in introns flanking alternatively spliced exons, enrichment in Alu sequences, which are frequently edited, may be involved in splicing regulation.

Cassette exons are ones which are not constitutively present in every transcript isoform derived from a gene. It has been reported that cassette exons are more edited than constitutive exons [23]. We therefore compared editing in cassette exons and constitutive exons in control cells and cells treated for 2 h. The data were normalized for the respective lengths of the inspected elements.

In control cells, we found cassette exons to be 1.56-fold richer in edited sites than constitutive exons in A549 and 1.76-fold richer in SH-SY5Y (p-values = 4×10^{-8} and $<2.2 \times 10^{-16}$, Figure 5C). In cells treated for 2 h, we found cassette exons to be 3.17-fold richer (A549) or 2.25-fold richer (SH-SY5Y) in edited sites than constitutive exons.

The complete dataset for 'alternative splicing events' is provided in Table S5.

Orthogonal validation of aberrant pre-mRNA splicing upon release of ADAR from the nucleolus

To obtain orthogonal confirmation of aberrant pre-mRNA splicing upon release of ADAR from the nucleolus and ensuing changes in editing, we validated directly, by differential RT-PCR, several exon-skipping and intron-retention events in SH-SY5Y cells. We chose these cells because the observed differences were more pronounced than in A549 cells (see below and Figure S11).

We examined exon skipping in two genes, ZNF217 and EIF4A2, as well as multiple intron retention events in MAT2A (Figure 6).

ZNF217 is an oncogene overexpressed in more than 10 cancer types. It is involved in cell proliferation and resistance to pro-apoptotic signals [52–56]. For ZNF217, on the basis of the sequencing data, rMATS computationally predicted reduced inclusion of exon 4 (see Figure 6A, reduction of inclusion level, 'IncLevel', from 0.89 to 0.67). To validate this by RT-PCR, we designed amplicons for detecting either exon 4 inclusion ('E4-E5', amplified with primers 2 and 3; and 'E3-E4-E5', amplified with primers 1 and 3) or exon 4 skipping ('E3-E5', amplified with primers 1 and 3) (Figure 6B).

Total RNA extracted from cells treated with Act D for 2 h and from untreated (control) cells was reverse transcribed and PCR amplified with different combinations of primers. At 2 h of treatment, the data clearly showed a decrease in E4-E5 amplicon (Figure 6B, lanes 2–3, product '**c**'), a decrease in E3-E4-E5 amplicon (Figure 6B, lanes 5–6, product '**a**'), and an increase in E3-E5 amplicon (Figure 6B, lanes 5–6, product '**b**'). These observations are all compatible with skipping of exon 4.

Interestingly, we noted that exon 4 of ZNF217 is flanked by head-to-head Alu sequences (AluSX1 and AluJb), which can interact by base-pairing to form a dsRNA, and whose editing strikingly increases upon treatment at 2 h (Figure S12A). Furthermore, using the Human Splicing Factor Database and SpliceAid [57], an algorithm assigning binding affinity scores to experimentally validated splicing factor-binding motifs, we found that increased editing of those Alu sequences generated regulatory elements promoting aberrant alternative splicing (Figure S12B). Indeed, editing in the AluSx1 element could disrupt sequence recognition by Sam68, hnRNP C1/C2, and HuB, thus repressing exon inclusion (Figure S12B, left), while editing in AluJb might promote exon exclusion by generating sequence recognition for the splicing regulatory factors SF2 and SRp55 (Figure S12B, right).

Also interesting, we detected fewer editing events in A549 cells than in SH-SY5Y cells in those Alu sequences in 2-h-treated samples, which is consistent with a lower level of exon 4 exclusion: from 0.88 to 0.75 in A549 cells (Figure S11A, left) instead of from 0.89 to 0.67 in SH-SY5Y cells (Figure S11A, right). Additionally, this figure shows a gradual reduction of the computed inclusion index over the time course, which speaks for the specificity of the effect.

We next focused on **EIF4A2**, a protein involved in colorectal cancer metastasis and drug resistance [58]. For EIF4A2, the computational prediction was reduced inclusion of exon 4, from 0.81 to 0.58 (Figure 6C). Here, RT-PCR performed with a combination of primers 1 and 3, used to amplify exon 3 spliced to exon 5, revealed in untreated cells a barely detectable amount of product (Figure 6D, lane 4), but abundant product after 2 h of treatment (Figure 6D, lane 5, product '**d**'). This attests to exon 4 skipping in treated cells. Note that for EIF4A2, amplification of all the other products was mildly increased at 2 h of treatment, as a result of increased expression (as *per* our RNAseq data, $\log_2$ FC = 0.8, q-value = 1.5×10^{-85}; see RPKM values in Figure 6C).

Finally, in case of **MAT2A**, a gene involved in transcriptional and metabolic reprogramming [59], the prediction was retention of three consecutive introns located between exons 6 and 9 (respective IncLevel increases from 0.10, 0.14, and 0.30 to 0.36, 0.43, and 0.57, Figure 6E). Targeting exons 6 and 7 for amplification with primers 3 and 4 gave rise to a short product that did not vary in abundance (spliced exons, product '**f**') and to larger products (unspliced/retained intron, product '**e**') showing a drastic increase in abundance after 2 h of treatment (Figure 6F, lanes 5–6). Similarly, primers 5 and 6, targeting exons 7 and 8, and primers 7 and 8, targeting exons 8 and 9, each detected a short product invariable in abundance (spliced exons, products '**d**' and '**b**') and larger products (unspliced, products 'c' and 'a') (Figure 6F, lanes 8–9 and lanes 11–12) which accumulated markedly in treated cells. As a further control, primers 1 and 2, targeting exons 2 and

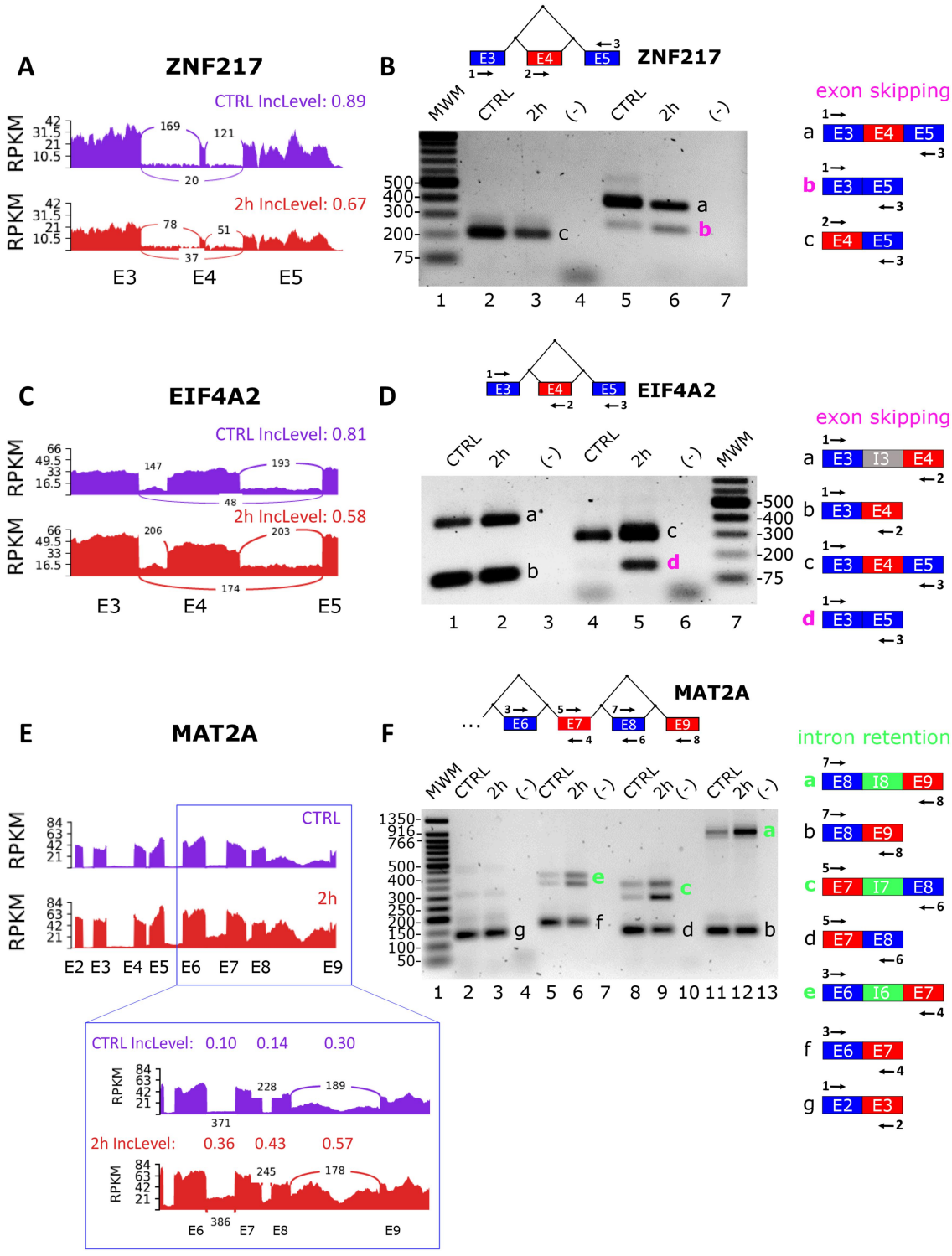

Figure 6. Validation of exon skipping and intron retention events by RT-PCR in SH-SY5Y Analysis of exon skipping and intron retention by deep sequencing and rMATS (panels A, C, and E) and by RT-PCR (B, D, and F). A-B) ZNF217, C-D) EIF4A2, E-F), MAT2A. rMATS analysis: the inclusion level (IncLevel) was computed as (I/LI) / (I/LI + S/LS), where I is the number of reads of the inclusion isoform, S the number of reads of the skipped isoform, LI the effective length of the inclusion isoform, and LS the effective length of the skipped isoform. RT-PCR analysis: samples loaded on a 2% agarose gel and stained with ethidium bromide. Negative control samples (-) consisted of PCR mix without cDNA. B), Size of PCR products: E4-E5 (product "c"), 207 bp; E3-E5 (product "b"), 270 bp; E3-E4-E5 (product "a"): 405 bp. D), Size of PCR products: E3-E4, 134 bp (product "b"); E3-intron-E4 (product "a"), 400 bp; E3-E5 (product "d"), 152 bp; E3-E4-E5 (product "c"), 292 bp. EIF4A2 overexpression (right, log2 FC = 0.8, q-value = 1.5x10-85). F), Size of PCR products: E2-E3 (product "g"), 134 bp; E6-E7 (product "f"), 169 bp; E6-intron-E7 (product "e"), 360 bp; E7-E8 (product "d"), 131 bp; E7-intron-E8 (product "c"), 249bp; E8-E9 (product "b"), 126 bp; E8-intron-E9 (product "a"), 761 bp. The reason why doublets are detected for amplification of E6-intron-E7 (lanes 5-6) and for E7-intron-E8 (lanes 8-9) are not clear and may indicate further regulation

3 (not predicted to undergo splicing regulation) amplified products whose abundance did not vary (Figure 6F, lanes 2 and 3, product 'g').

In conclusion, these results validate orthogonally the exon skipping and intron retention events predicted bioinformatically on the basis of the RNAseq data.

Discussion

Considering the number of gene expression steps and the range of normal and pathological processes impacted by A-to-I editing [60,61], it is of paramount importance to understand how ADAR is regulated in cells. RNA editing may cause alteration of the structure and stability of RNA duplexes [62], and, as shown here and elsewhere [22], alternative splicing regulation is a prime target.

ADAR could be regulated globally via control of its synthesis, metabolic stability, or activity, and this might involve post-translational modification. There is evidence of each of these possibilities: 1) in glioma cells, PTB1 positively modulates translation of ADAR p110 mRNA through an alternative mechanism of translation initiation [63] 2) in muscle tissue, AIMP2 acts as a negative regulator of editing by enhancing degradation of both ADAR isoforms and of ADARB1 [64] 3) AKT-dependent phosphorylation of both ADAR p110 and ADARB1 decreases deaminase activity in NB4 and CCRF-EM leukaemia cell lines [65].

ADAR could also be regulated locally, for instance via controlled access to specific substrates. Since RNA duplex formation is a prerequisite for ADAR editing activity, any factor that interferes with dsRNA formation and/or stability – such as association of an RNA-binding protein – could potentially influence editing at the local level.

It is quite remarkable that ADAR p150, but not ADAR p110, is well established to be induced by interferon [10] and that conversely, the nucleoli of numerous types of healthy and cancer cells are rich in ADAR p110 but not in ADAR p150. This prompted us to investigate if the membraneless nature of the nucleolus might be involved in regulating ADAR p110 activity, possibly via temporary sequestration of the protein.

The nucleolus is a multilayered biomolecular condensate formed by liquid–liquid phase separation and other phase transitions [29]. The nucleolus results from the act of 'making a ribosome', which begins at the core of the organelle with synthesis of ribosomal RNA precursors by RNA polymerase I. Precursor ribosomal RNAs act as a seed to promote condensate formation through gradual recruitment of ribosomal proteins and assembly factors to nascent ribosomal subunits. The nucleolus is organized in subphases maintained by rich networks of multivalent weak interactions between components. It is traversed constantly by molecules whose residency time within the organelle depends on their biochemical properties and their potential to mix with the phase. We reasoned that just as the nucleolus appears to sequester such molecules temporarily away from the nucleoplasm, it might act similarly in the case of ADAR.

Release of nucleolar ADAR increases RNA editing globally

In this study, we first confirmed in two cell lines, A549 and SH-SY5Y, the presence of ADAR in the nucleolus (Figure 1). In both cell lines, the p110 isoform is the dominantly expressed form. We hypothesized that we might explore the possible regulatory role of nucleolar enrichment in ADAR by gradually releasing it into the nucleoplasm and systematically assessing the consequences on RNA editing by deep transcriptome sequencing. To achieve this, we briefly treated cells with low doses of actinomycin D, known to induce nucleolar disassembly. Importantly, we used drug doses sufficient to inhibit RNA polymerase I (Pol I) without affecting Pol II or Pol III, and we monitored RNA editing shortly after treatment to minimize collateral effects (see paragraph on limitations below).

We found the nucleolus, in the steady state, to be particularly rich in ADAR. After 30 min of treatment, ADAR became abundant in the nucleoplasm, and by 60 min and beyond, it was almost exclusively present in the nucleoplasm with marked exclusion from the nucleolus (Figure 1A). Concurrently, we observed a significant increase in both the number of edited sites and the editing frequency (Figure 2).

Interestingly, an extensive literature search revealed that 20 years ago, at a time when the type of deep sequencing used here did not exist, a team applied a similar approach in mouse and rat cells (using NIH 3T3 and C6 glioma cells, respectively). They concluded that the translocation of ADARB1 from the nucleolus to the nucleoplasm was accompanied by an increase in RNA editing [32]. While only two edited sites were tested at the time (thousands here) by primer extension, the study reported a 30% increase in editing of ADARB1 pre-mRNA in NIH 3T3 cells and a 46% increase in editing of endogenous GluR-B pre-mRNAs in C6 glioma cells. Our work confirms but also considerably expands upon this pioneering study, providing a transcriptome-wide perspective on the original observations and analysing the consequences for differential pre-mRNA splicing. Additionally, we have conducted our experiments on two different cell lines (human).

Increased RNA editing occurs in introns and repetitive elements

Next, we investigated the editing targets of ADAR released from the nucleolus. The substrate specificity of the p110 and p150 isoforms of ADAR was investigated in mouse embryonic fibroblasts (MEFs) and HEK293 cells [50]. Specifically, RIP-seq experiments on HEK293 cells and ADAR isoform overexpression in ADAR$^{-/-}$ and ADARB1$^{-/-}$ MEFs revealed that ADAR p110 editing occurs mostly in intronic and repetitive regions, while ADAR p150 targets exonic and 3' UTR regions [50].

Our data revealed increased editing in intronic and repetitive sequences, thus incriminating ADAR p110 as the main contributor (Figure 3A). In addition, the increase in editing levels was mostly observed in 'unspliced reads' (Figure 3B-C). This suggests a co-transcriptional editing mechanism, consistent with the nuclear location of ADAR p110 and with its editing activity on pre-mRNAs and nascent RNAs near nucleoplasmic transcription sites. Altogether, our results are thus consistent with both ADAR p110 nuclear location and the known ADAR p110 editing specificity.

As the increase in editing observed upon release of ADAR from the nucleolus occurs co-transcriptionally, and hence prior to RNA splicing, we looked into regulation of alternative splicing by ADAR p110.

Several mechanisms have been proposed to explain how ADAR activity might influence splicing, which involve

binding of the protein and/or its editing activity [25]. For example, ADAR may regulate splicing by 'competing off' binding of splicing factors or by altering splicing sites normally recognized by splicing factors.

Our data reveal preferential editing in intronic sequences flanking cassette exons, along with enrichment of these sequences in Alu elements.

This led us to suggest that Alu editing might regulate alternative splicing (Figure S12). Previously, the potential role of Alu elements in alternative splicing regulation was studied in 293T cells [66]. It was notably shown that transfecting cells with a RABL5 minigene lacking intronic Alu elements resulted in a shift from alternative to constitutive inclusion of a downstream exon, highlighting a function of Alu elements in the regulation of splicing [66]. We proposed additionally that intronic editing might modulate splicing by generating or disrupting motif sequences targeted by *trans*-acting splicing factors (Figure S12B). Tang S. *et al.* transfected HEK293T cells with a CCDC15 minigene allowing or not intronic editing near CCDC15 exon 9. Intronic editing resulted in an increased binding affinity of SRSF7, promoting CCDC15 exon 9 skipping [25]. Altogether, these experimental results are in line with our computational approach and suggest that both Alu elements and editing may regulate alternative splicing functions.

In light of these observations, we searched for consensus motifs surrounding sites that exhibited increased editing following Act D treatment (Figure S13). Unsurprisingly, the top five motifs were shared between the two cell lines used in this study and largely corresponded to Alu elements (Figure S13A). Notably, a putative binding site for HuR, a protein involved in mRNA stability regulation and potentially interacting with ADAR [24], was also identified (Figure S13A).

To eliminate Alu-specific signals, we repeated the motif analysis using Alu sequences as the background instead of random sequences. This approach revealed cell-line specific motifs, whose biological relevance remains to be determined (Figure S13B).

We wondered if, in addition to altering *cis*-acting elements important for splicing, editing might also lead to changes in the production of *trans*-acting factors (i.e. splicing factors) themselves. To test this possibility, we performed a pathway enrichment analysis of genes with significant exon skipping or inclusion. Interestingly, we detected in both cell lines an enrichment in genes involved in splicing functions (first category affected, see Figure S14). We thus suggest that some of the reported effects on alternative splicing might be due to amplification caused by changed production of splicing factors.

Overexpression of ADAR and its release from the nucleolus both cause increased RNA editing

It is remarkable that the changes in RNA editing observed upon nucleolar disassembly appear quite similar to those observed when expression of ADAR is increased. For example, it has been reported that ADAR overexpression in breast cancer cells leads to an increase in editing frequency [33]. Interestingly, when we re-analysed RNA-seq data from ADAR-overexpressing EndoC-βH1 and HEK293 cell lines, we found intronic regions and cassette exons to be enriched in editing [67,68] (Figure S15A-B). Nucleolar disassembly led to very similar observations. This strengthens our hypothesis of global regulation of editing through nucleolar sequestration.

Limitations of the Study

This study provides novel insights into the global regulation of ADAR p110 activity through nucleolar sequestration. However, due to the pharmacological treatment we used – actinomycin D – this model has several limitations. Specifically: 1) many more proteins, beyond those investigated here (ADAR and ADARB1), are released from the nucleolus when it disassembles – nonetheless it is ADAR that carries the editing activity, 2) the transcription of many genes, in addition to rDNA, may potentially be affected by the treatment – we showed this is hardly the case at the drug concentration we used (Figure S7), and 3) the segregation of nucleolar components is accompanied by loss of ribosome production, which will inevitably impact protein synthesis. To minimize these collateral effects as much as possible, we have employed the following strategies: 1) we used low doses of actinomycin D, known to selectively inhibit Pol I-mediated transcription, and 2) we monitored RNA editing globally shortly after the start of treatment (as early as 30 min and not beyond 2 h). This time frame appears reasonable, considering that ribosomes are highly stable nanomachines with half-lives exceeding several days [69,70]. While our experimental and bioinformatic analyses clearly identify ADAR p110 as a major contributor to the effects observed upon nucleolar disassembly, we cannot completely rule out a contribution of ADARB1. Finally, an interesting internal control was provided by APOBEC editing that did not vary during our analysis (Figure S5).

A central finding of this study is the increase in RNA editing observed following the release of ADAR from the nucleolus – where it has no known substrates – into the nucleoplasm, which harbours numerous editing targets. This redistribution correlates with splicing alterations, consistent with previous studies linking elevated A-to-I editing to changes in splicing patterns of the type reported here. We therefore consider it likely that the splicing aberrations observed result, at least in part, from increased ADAR activity in the nucleoplasm. Nevertheless, we cannot formally exclude the possibility that the treatment itself may contribute to some extent to the observed splicing defects.

Conclusions

What might be the implications of the main conclusion of this work, namely that a significant fraction of ADAR is retained in the nucleolus so as to restrict its activity? Firstly, a prediction of our model is that ADAR-mediated RNA editing should be regulated during the cell cycle. The nucleolus is disassembled at every cell cycle, breaking

down at the onset of mitosis and forming again at the end of mitosis [29]. This implies that nucleolus-restricted ADAR is 'out' at least a fraction of the time during the cell cycle. Secondly, our findings shed new light on how alterations in RNA editing may contribute to various diseases, including cancer and neurodegeneration [60,61]. These are often associated with significant alterations in nucleolar structure [71,72], which could affect the normal kinetics of ADAR retention in the nucleolus, leading to its partial release.

Materials and methods

All reagents used listed in Table 1.

Cell culture

The A549 cell line (CCL-185) was purchased from ATCC and cultured in DMEM supplemented with 10% FBS and 1% penicillin/streptomycin. The SH-SY5Y cell line was a kind gift from Dr Sajid Muhamad (Germany) and was cultured in DMEM supplemented with 15% FBS and 1% penicillin/streptomycin. All cell lines were maintained at 37°C under 5% CO_2.

Nucleolar disassembly

For microscopy imaging, 20,000 cells were plated in a 96-well glass-bottom PORVAIR plate. For the extraction of protein and RNA, 600,000 cells were plated in a 6-well plate for 24 h. In order to trigger nucleolar disassembly, cells were cultured in a fresh medium supplemented with actinomycin D at 0.1 µg/mL for 30, 60, 90, or 120 min.

Immunofluorescence

Following actinomycin D treatment, the cells were immediately fixed with 4% paraformaldehyde and washed with PBS. They were then permeabilized and blocked with 1% PBS/BSA/0.3% Triton for 1 h at room temperature. They were then incubated with primary antibodies against ADAR, ADARB1, PES1, and fibrillarin overnight at 4°C. Following three 10-min washes with PBS, incubation with secondary antibodies was carried out for 1 h at room temperature, concomitantly with DAPI staining. Following three 10-min washes with PBS, images were captured by spinning-disc confocal microscopy (63× objective).

Western blotting

Following actinomycin D treatment, cells were detached with 0.5 mm EDTA/PBS and centrifuged for 5 min at 500 g. Cell pellets were lysed in buffer containing 50 mm Tris/HCl, 250 mm NaCl, 500 mm EDTA, 0.5% igepal, and 10% glycerol. Ten micrograms of total protein lysate was resolved on an 8% acrylamide gel and transferred to a nitrocellulose membrane. Membranes were blocked with 5% milk/TBS-T and incubated with primary antibodies overnight at 4°C. Membranes were washed in TBS-T and incubated for 1 h at room temperature with HRP-coupled secondary antibodies. Proteins were revealed by chemiluminescence after three TBS-T washes.

RT-PCR

Total RNA (4 µg) extracted from untreated or 2-h Act D-treated SH-SY5Y cells was incubated with 1 µl DNase

Table 1. Reagents.

Reagent/Resource	Reference or Source	Identifier or Catalog Number	
Cell lines			
A549	ATCC	CCL-185	
SH-SY5Y	Gift from Prof. Sajid Muhamad (U. Cologne, Germany)		
Reagents			
Actinomycin D	A1410	Sigma	Used at 0.1 µg/mL for 30, 60, 90 or 120 min
Supersignal west pico plus	34580	ThermoFisher	
DMEM	BE12-604F	Lonza	
FBS	F7524	Sigma	
Penicillin-Streptomycin	DE17-602E	Lonza	
RNA 6000 Nano Kit	#5067–1511	Agilent	
DNase I	18068015	ThermoFisher	
DNase I buffer 10X	10640226	Invitrogen	
SuperScript III	11752–050	Invitrogen	
GoTaq Flexi Buffer 5X	M890A	Promega	
MgCl2	A351H	Promega	
GoTaq G_2 Flexi	M7808	Promega	
Antibodies			Dilutions used:
Anti-ADAR (E6X9R) rabbit	81284S	Cell Signaling	WB: 1/1000
Anti-ADARB1 from mouse	SAB1405426	Sigma	IF: 1/500, WB: 1/1000
Anti-PES1 from rat		IMI Munich E.Kremmer	IF: 1/1000
Anti-Fibrillarin from rabbit	ab5821	Abcam	IF: 1/1000
Anti-Actin (AC15) from goat	SC 69,879	Santa Cruz	WB: 1/1000
HRP Anti-rabbit from goat	NA934V	Amersham	WB: 1/2000
HRP Anti-mouse from goat	115–035–062	Jackson immunoreserach	WB: 1/2000
Alexa 488 anti-rabbit from chicken	A21441	Invitrogen	IF: 1/1000
Alexa 488 anti-mouse from goat	A11001	Invitrogen	IF: 1/1000
Alexa 568 anti-rat from goat	A11077	Invitrogen	IF: 1/1000

Table 2. Primers used in RT-PCR.

		Sequence	Annealing temperature
MAT2A			
Amplicon 2–3	Forward	5′-ACCAAATCAGTGATGCTG-3′	53°C
	Reverse	5′-TAGTCAACAGCAGCTCTG-3′	
Amplicon 6–7	Forward	5′-AATCTACCACCTACAGCC-3′	55°C
	Reverse	5′-ATAAGCAGCTGAACGGTC-3′	
Amplicon 7–8	Forward	5′-TGCTTATGCTGCTCGTTG-3′	55°C
	Reverse	5′-AGGTACCATAATGGAAAATGG-3′	
Amplicon 8–9	Forward	5′-AGAGTGAGAGAGAGCTATTAG-3′	53°C
	Reverse	5′TACCAAAGTGGCCATAGG-3′	
ZNF217			
Amplicon 3–5	Forward	5′-TCAGTAGCTTTCACCATTCGC-3′	57°C
	Reverse	5′-AGGCATCACATCACTGTTACC-3′	
Amplicon 4–5	Forward	5′-TCAGTAGCTTTCACCATTCGC-3′	54°C
	Reverse	5′-AGGCCTGTGTCATATCAAC-3′	
EIF4A2			
Amplicon 3–5	Forward	5′-TGGCATCTATGCTTACGG-3′	50°C
	Reverse	5′-ATTTCGAACATTTGTTCCACC-3′	
Amplicon 3–4	Forward	5′-TGGCATCTATGCTTACGG-3′	54°C
	Reverse	5′-ATGGAAATAGCAAATGTGGC-3′	

I for 30 min, prior to the addition of 1 µl stop buffer and further incubation at 65°C for 10 min. Five micrograms of DNase I-treated RNA was next treated with 2 µl SuperScript III reverse transcriptase and 10 µL SuperMix 2. In the negative reaction mix, 15 µl DEPC was added to 5 µl DNase I-treated RNA. Samples were next incubated in an Applied Biosystems PCR cycler with the following programme: 10 min at 25°C, 30 min at 50°C, 5 min at 85°C, 5 min at 4°C with addition of 1 µl RNase, 20 min at 37°C.

PCR mix was prepared with 30 µl GoTaq Flexi Buffer 5X, 12 µl $MgCl_2$, 3 µl dNTPs, 4.5 µl forward and reverse primers. Five microlitres of cDNA was treated with 0.75 µl GoTaq G2 Flexi polymerase and 45 µl PCR mix. Negative control samples consisted of 45 µl PCR mix and 5 µl H_2O. Twenty microlitres of treated cDNA was loaded into the PCR cycler with the following programme: 5 min at 95°C, 20 s at 95°C, an annealing step for 30 s (see temperature below), 1 min at 72°C (the last three steps were repeated 35 times) and 10 min at 72°C. Twelve microlitres of each PCR sample was loaded for migration on a 2% agarose gel with TAE 1X. All primers used listed in **Table 2.**

RNA extraction and RNA sequencing

Following actinomycin D treatment, cells were treated with TRI reagent, and RNA was extracted according to the manufacturer's procedure. RNA integrity and purity were checked by Agilent analysis. RNA libraries were pooled and sequenced using the 101-base paired-end option with the Illumina NovaSeq 6000 system (BRIGHTCore, Brussels, Belgium).

Sequenced read quality was assessed with FastQC (0.11.9). Reads were trimmed of adapters and for quality with Trimmomatic (0.39), with the default parameters. Trimmed reads were aligned on the human genome V19 (hg19) with STAR (2.7.10b). Up to three mismatches were allowed, depending on mapped read length. Multi-mapped reads were discarded in subsequent analyses. Aligned SAM files were sorted and converted to BAM files with SAMtools (1.14). PCR duplicate reads were marked with SAMtools.

Editing detection

RNA editing was detected with REDItools (1.0.4). REDItools detects adenosine-to-inosine conversion by combining DNA-seq and RNA-seq alignment in BAM format.

Whole-genome sequencing reads from A549, K562, and HEK293 cells were downloaded in fastq format (cf. Statistical analysis). WGS reads were mapped to the human reference genome hg19 with bwa (0.7.17) (default parameters) and converted to BAM with SAMtools (1.14).

We used the REDItoolDnaRna.py script to detect editing events in RNA-seq data and to filter out SNPs from the corresponding cell-line genome. Reads with a Phred score <25 were filtered out in DNA-seq and RNA-seq. Reads marked as duplicated in DNA-seq and RNA-seq were excluded. For paired-end reads, only concordant reads were used. For strand-specific sequencing libraries, editing sites were inferred according to the read strand. A strand correction was applied to remove sites detected on the opposite strand.

For SH-SY5Y, HUES9, and EndoC-βH1, we used REDItoolsDenovo.py script to detect editing sites without DNA-seq data. A known database of SNPs of the SH-SY5Y cell line was used to filter out false positives detected with REDItoolsDenovo.py. For HUES9 and EndoC-βH1, only editing sites detected in the REDIportal database were selected for further analysis.

RNA/DNA mismatch detection

To ensure consistency with editing detection, all RNA/DNA mismatches were computed as described in the *Editing detection* section.

Motif discovery

Enriched motifs were identified using HOMER (v5.1). The initial analysis was performed using random genomic sequences as the background. A second analysis was then conducted using Alu sequences as background to eliminate Alu-specific signals and reveal novel motifs.

Differential expression analysis

Transcript counts were estimated with featureCounts (1.5.1) in the paired-end and reversely stranded modes. Reads were assigned to features with the hg19 annotation file (*gencode.v19.annotation.gtf*) from GENCODE project. Quantification of isoforms was performed with RSEM (1.3.3) in the paired-end and reverse-stranded modes. Differential expression analysis of genes and isoforms was performed with DESeq2.

Alternative splicing events

Alternative splicing events were detected with rMATS (4.0.7), with parameters enabling clipping and variable read lengths. rMATS computes the difference in inclusion level between the two conditions, computed as Inclusion Level = (I/LI)/(I/LI + S/LS) where I is the number of reads of the inclusion isoform, S is the number of reads of the skipping isoform, L_i is the effective length of the inclusion and isoform, L_s is the effective length of the skipping isoform. In both exon skipping and intron retention events, the effective lengths L_i and L_s are computed as $L_i = 2(j - r + 1)$ and $L_s = j - r + 1$, where j is the junction length and r is the read length.

Unspliced and spliced read extraction

To investigate whether editing occurs co-transcriptionally, we used SAMtools (1.14) to split the RNA-seq data into spliced and unspliced reads. Spliced reads were extracted according to the presence of the N tag in the CIGAR (Compact Idiosyncratic Gapped Alignment Report). In a SAM file, the CIGAR consists of a chain of characters defining how a read aligns to the reference genome. The N character stands for 'no query base to align' and hence for a read gap corresponding to a spliced read. We used the GENCODE annotation file to keep only reads overlapping exons. Unspliced reads were extracted according to the absence of the N tag in the CIGAR. We used the GENCODE annotation file to keep reads overlapping both exon and intron regions.

Statistical analysis

Computations were implemented with R programming language (4.2.3) and RStudio (2023.03.0, Build 386). Data processing was performed with data.table (1.14.8), dplyr (1.1.1), plyr (1.8.8) and stringr (1.5.0). Editing events were annotated with GenomicRanges (1.48.0). Figures were generated with the ggplot2 library (3.4.2).

Statistical tests (Chi-squared test, Fisher's exact test, *p*-values, *q*-values, Wilcoxon test, t-test) were computed with the R programming language (4.2.3).

Acknowledgments

We express our profound gratitude to Ludivine Wacheul (ULB, RNA Molecular Biology) for her invaluable support throughout the course of this project.

Disclosure statement

No potential conflict of interest was reported by the author(s).

Funding

R.L. was supported by Fonds de la Recherche Scientifique (FRIA). Research in the Lab of V.D. was supported by the Belgian Fonds de la Recherche Scientifique (F.R.S./FNRS), the Fondation Belge contre le cancer, and an ARC grant from the Université libre de Bruxelles. Research in the Lab of D.L.J.L. was supported by the Belgian Fonds de la Recherche Scientifique (F.R.S./FNRS), EOS [CD-INFLADIS, grant n° 40007512], Région Wallonne (SPW EER) Win4SpinOff [RIBOGENESIS], the COST actions EPITRAN (CA16120) and TRANSLACORE (CA21154), the European Joint Programme on Rare Diseases (EJP-RD) RiboEurope and DBAGeneCure.This article is based upon work from COST Action CA21154 TRANSLACORE, supported by COST (European Cooperation in Science and Technology).

Authors contributions

R.L. conducted all bioinformatic analyses and performed orthogonal validation of differential splicing using RT-PCR. R.B. carried out the nucleolus disassembly assays, prepared RNA samples, assessed ADAR levels via Western blotting, and performed immunofluorescence analyses. V.D. and D.L.J.L. conceptualized and designed the project, secured funding and managed the research. All authors contributed to drafting the manuscript, while D.L.J.L. finalized and submitted it. D.L.J.L. revised the manuscript. All authors have reviewed and approved the final version of the manuscript.

Annotation files

Annotation files of intronic (*intronic.annotation.hg19.bed*), 3'UTR (*3UTR.annotation.hg19.bed)*, 5'UTR regions (*5UTR.annotation.hg19.bed)*, repetitive elements (*repetitive.repeatmasker.hg19.gtf*), and human reference genome hg19 (*hg19.fa*) were downloaded from the UCSC genome browser (http://genome.ucsc.edu). The comprehensive annotation file of the human reference genome v19 was downloaded from the GENCODE project (https://www.gencodegenes.org/). Annotations of cassette (*hg19_cassette_exons_annotation.txt)* and constitutive exons (*hg19_constitutive_exons_annotation.txt*) were downloaded in the splicing exon event database HEXEvent (https://hexevent.mmg.uci.edu/).

Data availibility

The data that support the findings of this study are openly available in [NCBI] at [https://www.ncbi.nlm.nih.gov/bioproject/1201561]. Tables S1-S5 are available at https://zenodo.org/records/15510922. Any further underlying data will be shared upon reasonable request.

Editing-related data

Whole-genome sequencing data for A549 were downloaded from the Cancer Cell Line Encyclopedia (CCLE). The K562 genome was downloaded from the ENCODE project (GSE177509). Known SNP events of the SH-SY5Y cell line were downloaded from Krishna A et al. (https://systemsbiology.uni.lu/shsy5y/). Human editing events were downloaded from the REDIportal database. These consisted of 16 million editing events from 9642 RNA-seq samples from the GTEx project (http://srv00.recas.ba.infn.it/atlas/).

RNA-seq data

Our analysis relied on the use of published available data:

- ADAR overexpression data for HEK293 and EndoC-βH1 were downloaded from the Gene Expression Omnibus (GEO) database from Song Y et al., Szymczak F et al. (GSE136326, GSE214851).
- ADAR p150 overexpression data for HEK293 were obtained from Sun T et al. (PRJNA590956).
- siRNA ADAR data for U87MG were downloaded from Bahn JH et al. (GSE28040).
- RIP-seq data of ADAR p110 and ADAR p150 were downloaded from Kleinova et al. (GSE188937).
- Actinomycin D-treated RNA-seq data in K562 and HUES9 were downloaded from Melé M et al. (GSE80046).

ORCID

Denis L. J. Lafontaine http://orcid.org/0000-0001-7295-6288

References

[1] Wagner RW, Smith JE, Cooperman BS, et al. A double-stranded RNA unwinding activity introduces structural alterat ions by means of adenosine to inosine conversions in mammalian cells and Xenopus eggs. In: Proceedings of the National Academy of Sciences of the United States of America; 1989. Vol. 86. p. 2647–2651.

[2] Polson AG, Crain PF, Pomerantz SC, et al. The mechanism of adenosine to inosine conversion by the double-strande d RNA unwinding/modifying activity: a high-performance liquid chromato graphy-mass spectrometry analysis. Biochemistry. 1991;30 (49):11507–11514. doi: 10.1021/bi00113a004

[3] Bass BL, Weintraub H. An unwinding activity that covalently modifies its double-stranded RNA substrate. Cell. 1988;55 (6):1089–1098. doi: 10.1016/0092-8674(88)90253-X

[4] Picardi E, Am D, Lo Giudice C, et al. Rediportal: a comprehensive database of A-to-I RNA editing events in h umans. Nucleic Acids Res. 2017;45(D1):D750–D7. doi: 10.1093/nar/gkw767

[5] Morse DP, Aruscavage PJ, Bass BL. RNA hairpins in noncoding regions of human brain and Caenorhabditis el egans mRNA are edited by adenosine deaminases that act on RNA. In: Proceedings of the National Academy of Sciences of the United States of America; 2002. Vol. 99. p. 7906–7911.

[6] Athanasiadis A, Rich A, Maas S, et al. Widespread A-to-I RNA editing of Alu-containing mRNAs in the human tra nscriptome. PLOS Biol. 2004;2(12):e391. doi: 10.1371/journal.pbio.0020391

[7] Kim DDY, Kim TTY, Walsh T, et al. Widespread RNA editing of embedded Alu elements in the human transcrip tome. Genome Res. 2004;14(9):1719–1725. doi: 10.1101/gr.2855504

[8] Levanon EY, Eisenberg E, Yelin R, et al. Systematic identification of abundant A-to-I editing sites in the huma n transcriptome. Nat Biotechnol. 2004;22(8):1001–1005. doi: 10.1038/nbt996

[9] Bazak L, Levanon EY, Eisenberg E. Genome-wide analysis of Alu editability. Nucleic Acids Res. 2014;42(11):6876–6884. doi: 10.1093/nar/gku414

[10] Patterson JB, Samuel CE. Expression and regulation by interferon of a double-stranded-RNA-speci fic adenosine deaminase from human cells: evidence for two forms of th e deaminase. Mol Cell Biol. 1995;15(10):5376–5388. doi: 10.1128/MCB.15.10.5376

[11] George CX, Samuel CE. Human RNA-specific adenosine deaminase ADAR1 transcripts possess alter native exon 1 structures that initiate from different promoters, one c onstitutively active and the other interferon inducible. In: Proceedings of the National Academy of Sciences of the United States of America; 1999. Vol. 96. p. 4621–4626.

[12] Kawakubo K, Samuel CE. Human RNA-specific adenosine deaminase (ADAR1) gene specifies transcri pts that initiate from a constitutively active alternative promoter. Gene. 2000;258(1–-2):165–172. doi: 10.1016/S0378-1119(00)00368-1

[13] Seeburg PH, Hartner J. Regulation of ion channel/neurotransmitter receptor function by RNA ed iting. Curr Opin Neurobiol. 2003;13(3):279–283. doi: 10.1016/S0959-4388(03)00062-X

[14] Jacobs MM, Fogg RL, Emeson RB, et al. ADAR1 and ADAR2 expression and editing activity during forebrain devel opment. Dev Neurosci. 2009;31(3):223–237. doi: 10.1159/000210185

[15] Nishikura K. Functions and regulation of RNA editing by ADAR deaminases. Annu Rev Biochem. 2010;79(1):321–349. doi: 10.1146/annurev-biochem-060208-105251

[16] Uhlén M, Fagerberg L, Hallström BM, et al. Tissue-based map of the human proteome. Science. 2015;347(6220):1260419. doi: 10.1126/science.1260419

[17] Melcher T, Maas S, Herb A, et al. RED2, a brain-specific member of the RNA-specific adenosine deaminase family*. J Biol Chem. 1996;271(50):31795–31798. doi: 10.1074/jbc.271.50.31795

[18] Chen CX, Cho DS, Wang Q, et al. A third member of the RNA-specific adenosine deaminase gene family, ADAR3, contains both single- and double-stranded RNA binding domains. Vol. 6. RNA (New York, NY; 2000. p. 755–767.

[19] Cho D-S, Yang W, Lee JT, et al. Requirement of dimerization for RNA editing activity of adenosine deam inases acting on RNA. J Biol Chem. 2003;278(19):17093–17102. doi: 10.1074/jbc.M213127200

[20] Savva YA, Rieder LE, Reenan RA. The ADAR protein family. Genome Biol. 2012;13(12):252. doi: 10.1186/gb-2012-13-12-252

[21] Raghava Kurup R, Oakes EK, Manning AC, et al. RNA binding by ADAR3 inhibits adenosine-to-inosine editing and promote s expression of immune response protein MAVS. J Biol Chem. 2022;298(9):102267. doi: 10.1016/j.jbc.2022.102267

[22] Rueter SM, Dawson TR, Emeson RB. Regulation of alternative splicing by RNA editing. Nature. 1999;399(6731):75–80. doi: 10.1038/19992

[23] Solomon O, Oren S, Safran M, et al. Global regulation of alternative splicing by adenosine deaminase actin g on RNA (ADAR). RNA. 2013;19(5):591–604. doi: 10.1261/rna.038042.112

[24] Wang S IX, E DJ, Zhao Y, et al. ADAR regulates RNA editing, transcript stability, and gene expression. Cell Rep. 2013;5 (3):849–860. doi: 10.1016/j.celrep.2013.10.002

[25] Tang SJ, Shen H, An O, et al. Cis- and trans-regulations of pre-mRNA splicing by RNA editing enzymes influence cancer development. Nat Commun. 2020;11(1):799. doi: 10.1038/s41467-020-14621-5

[26] Liddicoat BJ, Piskol R, Chalk AM, et al. RNA editing by ADAR1 prevents MDA5 sensing of endogenous dsRNA as nons elf. Sci (New York, NY). 2015;349(6252):1115–1120. doi: 10.1126/science.aac7049

[27] Rice GI, Kasher PR, Forte GMA, et al. Mutations in ADAR1 cause aicardi-goutières syndrome associated with a type I interferon signature. Nat Genet. 2012;44(11):1243–1248. doi: 10.1038/ng.2414

[28] Mannion NM, Greenwood SM, Young R, et al. The RNA-Editing enzyme ADAR1 controls innate immune responses to RNA. Cell Rep. 2014;9(4):1482–1494. doi: 10.1016/j.celrep.2014.10.041

[29] Lafontaine DLJ, Riback JA, Bascetin R, et al. The nucleolus as a multiphase liquid condensate. Nat Rev Mol Cell Biol. 2021;22 (3):165–182. doi: 10.1038/s41580-020-0272-6

[30] Desterro JMP, Keegan LP, Lafarga M, et al. Dynamic association of RNA-editing enzymes with the nucleolus. J Cell Sci. 2003;116 (9):1805–1818. doi: 10.1242/jcs.00371

[31] Vitali P, Basyuk E, Le Meur E, et al., et al. ADAR2-mediated editing of RNA substrates in the nucleolus is inhibited by C/D small nucleolar RNAs. Journal Cell Biology. 2005;169(5):745–753. doi: 10.1083/jcb.200411129

[32] Sansam CL, Wells KS, Emeson RB. Modulation of RNA editing by functional nucleolar sequestration of ADA R2. In: Proceedings of the National Academy of Sciences of the United States of America; 2003. Vol. 100. p. 14018–14023.

[33] Fumagalli D, Gacquer D, Rothé F, et al. Principles governing A-to-I RNA editing in the breast cancer transcrip tome. Cell Rep. 2015;13(2):277–289. doi: 10.1016/j.celrep.2015.09.032

[34] Nie Y, Zhao Q, Su Y, et al. Subcellular distribution of ADAR1 isoforms is synergistically Determin ed by three nuclear discrimination signals and a regulatory motif*. J Biol Chem. 2004;279 (13):13249–13255. doi: 10.1074/jbc.M312753200

[35] Chilibeck KA, Wu T, Liang C, et al. FRET analysis of in vivo dimerization by RNA-editing enzymes*. J Biol Chem. 2006;281 (24):16530–16535. doi: 10.1074/jbc.M511831200
[36] Frassinelli L, Orecchini E, Al-Wardat S, et al. The RNA editing enzyme ADAR2 restricts L1 mobility. RNA Biol. 2021;18 (sup1):75–87. doi: 10.1080/15476286.2021.1940020
[37] Díaz-Piña G, Rubio K, Ordoñez-Razo RM, et al. ADAR1 isoforms regulate let-7d processing in idiopathic pulmonary fibr osis. Int J Mol Sci. 2022;23(16):9028. doi: 10.3390/ijms23169028
[38] Freund EC, Sapiro AL, Li Q, et al. Unbiased identification of trans regulators of ADAR and A-to-I RNA edi ting. Cell Rep. 2020;31 (7):107656. doi: 10.1016/j.celrep.2020.107656
[39] Cottrell KA, Ryu S, Torres LS, et al. Induction of viral mimicry upon loss of DHX9 and ADAR1 in breast cancer cells. Cancer Res. Commun. 2024;4(4): 986–1003. doi:10.1158/2767-9764.CRC-23-0488
[40] Vukic D, Cherian A, Keskitalo S, et al. Distinct interactomes of ADAR1 nuclear and cytoplasmic protein isoforms and their responses to interferon induction. Nucleic Acids Res. 2024;52 (22):14184–14204. doi: 10.1093/nar/gkae1106
[41] Perry RP, Kelley DE. Inhibition of RNA synthesis by actinomycin D: characteristic dose-resp onse of different RNA species. J Cell Physiol. 1970;76(2):127–139. doi: 10.1002/jcp.1040760202
[42] Ghoshal K, Jacob ST. Specific inhibition of pre-ribosomal RNA processing in extracts from the lymphosarcoma cells treated with 5-fluorouracil. Cancer Res. 1994;54(3):632–636.
[43] Haaf T, Ward DC. Inhibition of RNA polymerase II transcription causes chromatin decondensation, loss of nucleolar structure, and dispersion of chromosomal domains. Exp Cell Res. 1996;224 (1):163–173. doi: 10.1006/excr.1996.0124
[44] Bensaude O. Inhibiting eukaryotic transcription: which compound to choose? How to evaluate its activity? Transcription. 2011;2(3):103–108. doi: 10.4161/trns.2.3.16172
[45] Ochs RL, Lischwe MA, Spohn WH, et al. Fibrillarin: a new protein of the nucleolus identified by autoimmune s era. Biol Cell. 1985;54 (2):123–133. doi: 10.1111/j.1768-322X.1985.tb00387.x
[46] Oeffinger M, Leung A, Lamond A, et al. Yeast pescadillo is required for multiple activities during 60S riboso mal subunit synthesis. RNA. 2002;8(5):626–636. doi: 10.1017/S1355838202020022
[47] Picardi E, Pesole G. Reditools: high-throughput RNA editing detection made easy. Bioinformatics. 2013;29(14):1813–1814. doi: 10.1093/bioinformatics/btt287
[48] Barretina J, Caponigro G, Stransky N, et al. The cancer cell line encyclopedia enables predictive modeling of antic ancer drug sensitivity. Nature. 2012;483(7391):603–607. doi: 10.1038/nature11003
[49] Krishna A, Biryukov M, Trefois C, et al. Systems genomics evaluation of the SH-SY5Y neuroblastoma cell line as a model for Parkinson's disease. BMC Genomics. 2014;15(1):1154. doi: 10.1186/1471-2164-15-1154
[50] Kleinova R, Rajendra V, Leuchtenberger AF, et al. The ADAR1 editome reveals drivers of editing-specificity for ADAR1-isoforms. Nucleic Acids Res. 2023;51(9):4191–4207. doi: 10.1093/nar/gkad265
[51] Shen S, Park JW, Z-X L, et al. rMATS: robust and flexible detection of differential alternative splic ing from replicate RNA-Seq data. In: Proceedings of the National Academy of Sciences; 2014. Vol. 111. p. E5593–E601.
[52] Banck MS, Li S, Nishio H, et al. The ZNF217 oncogene is a candidate organizer of repressive histone mod ifiers. Epigenetics. 2009;4(2):100–106. doi: 10.4161/epi.4.2.7953
[53] Ginestier C, Cervera N, Finetti P, et al. Prognosis and gene expression profiling of 20q13-amplified breast canc ers. Clin Cancer Res: An Off J Am Associat Ion For Cancer Res. 2006;12 (15):4533–4544. doi: 10.1158/1078-0432.CCR-05-2339
[54] Krig SR, Miller JK, Frietze S, et al. ZNF217, a candidate breast cancer oncogene amplified at 20q13, regulat es expression of the ErbB3 receptor tyrosine kinase in breast cancer c ells. Oncogene. 2010;29(40):5500–5510. doi: 10.1038/onc.2010.289
[55] Thollet A, Vendrell JA, Payen L, et al. ZNF217 confers resistance to the pro-apoptotic signals of paclitaxel a nd aberrant expression of aurora-A in breast cancer cells. Mol Cancer. 2010;9(1):291. doi: 10.1186/1476-4598-9-291
[56] Bellanger A, Le DT, Vendrell J, et al. Exploring the significance of the exon 4-skipping isoform of the ZNF21 7 oncogene in breast cancer. Front Oncol. 2021;11:11. doi: 10.3389/fonc.2021.647269
[57] Giulietti M, Piva F, D'Antonio M, et al. SpliceAid-F: a database of human splicing factors and their RNA-bindin g sites. Nucleic Acids Res. 2013;41:D125–D31.
[58] Chen ZH, Qi JJ, Wu QN, et al. Eukaryotic initiation factor 4A2 promotes experimental metastasis and oxaliplatin resistance in colorectal cancer. J Exp Clin Cancer Res. 2019;38(1):196. doi: 10.1186/s13046-019-1178-z
[59] Chen H, Xia M, Lin M, et al. Role of methionine adenosyltransferase 2A and S-adenosylmethionine in mitogen-induced growth of human colon cancer cells. Gastroenterology. 2007;133 (1):207–218. doi: 10.1053/j.gastro.2007.03.114
[60] Gallo A, Vukic D, Michalik D, et al. ADAR RNA editing in human disease; more to it than meets the I. Hum Genet. 2017;136(9):1265–1278. doi: 10.1007/s00439-017-1837-0
[61] Baker AR, Slack FJ. ADAR1 and its implications in cancer development and treatment. Trends Genet. 2022;38(8):821–830. doi: 10.1016/j.tig.2022.03.013
[62] Mendoza HG, Beal PA. Structural and functional effects of inosine modification in mRNA. RNA. 2024;30(5):512–520. doi: 10.1261/rna.079977.124
[63] Yang B, Hu P, Lin X, et al. PTBP1 induces ADAR1 p110 isoform expression through IRES-like dependen t translation control and influences cell proliferation in gliomas. Cellular And Mol Life Sci. 2015;72(22):4383–4397. doi: 10.1007/s00018-015-1938-7
[64] Tan MH, Li Q, Shanmugam R, et al. Dynamic landscape and regulation of RNA editing in mammals. Nature. 2017;550 (7675):249–254. doi: 10.1038/nature24041
[65] Bavelloni A, Focaccia E, Piazzi M, et al. AKT-dependent phosphorylation of the adenosine deaminases ADAR-1 and - 2 inhibits deaminase activity. FASEB J: Off Publ Fed Am Soci Eties For Exp Biol. 2019;33(8):9044–9061. doi: 10.1096/fj.201800490RR
[66] Lev-Maor G, Ram O, Kim E, et al. Intronic alus influence alternative splicing. PLOS Genet. 2008;4(9):e1000204. doi: 10.1371/journal.pgen.1000204
[67] Szymczak F, Cohen-Fultheim R, Thomaidou S, et al. ADAR1-dependent editing regulates human β cell transcriptome diversity during inflammation. Front Endocrinol (Lausanne). 2022;13. doi: 10.3389/fendo.2022.1058345
[68] Song Y, Yang W, Fu Q, et al. irCLASH reveals RNA substrates recognized by human ADARs. Nat Struct & Mol Biol. 2020;27 (4):351–362. doi: 10.1038/s41594-020-0398-4
[69] Nikolov EN, Dabeva MD, Nikolov TK. Turnover of ribosomes in regenerating rat liver. Int J Biochem. 1983;15(10):1255–1260. doi: 10.1016/0020-711X(83)90215-X
[70] Hirsch CA, Hiatt HH. Turnover of liver ribosomes in Fed and in fasted rats. J Biol Chem. 1966;241(24):5936–5940. doi: 10.1016/S0021-9258(18)96360-X
[71] Montanaro L, Treré D, Nucleolus DM. Ribosomes, and cancer. Am J Pathol. 2008;173(2):301–310. doi: 10.2353/ajpath.2008.070752
[72] Corman A, Sirozh O, Lafarga V, et al. Targeting the nucleolus as a therapeutic strategy in human disease. Trends Biochem Sci. 2023;48(3):274–287. doi: 10.1016/j.tibs.2022.09.006